Petrology of the Eagle Sandstone, Bearpaw Mountains Area, North-Central Montana

GEOLOGICAL SURVEY BULLETIN 1521

Prepared in cooperation with the U.S. Department of Energy

Petrology of the Eagle Sandstone, Bearpaw Mountains Area, North-Central Montana

By DONALD L. GAUTIER

INVESTIGATIONS OF SHALLOW GAS RESERVOIRS IN THE NORTHERN GREAT PLAINS

GEOLOGICAL SURVEY BULLETIN 1521

Prepared in cooperation with the U.S. Department of Energy

Composition and burial history of an important conventional shallow methane reservoir in the northern Great Plains

UNITED STATES GOVERNMENT PRINTING OFFICE, WASHINGTON : 1981

UNITED STATES DEPARTMENT OF THE INTERIOR

JAMES G. WATT, *Secretary*

GEOLOGICAL SURVEY

Dallas L. Peck, *Director*

Library of Congress Cataloging in Publication Data
Gautier, Donald L.
Petrology of the Eagle Sandstone, Bearpaw Mountains area, north-central Montana.
(Investigations of shallow gas reservoirs in the northern Great Plains)
(Geological Survey Bulletin 1521)
Bibliography: p. 52
1. Sandstone–Montana–Bearpaw Mountains region. 2. Gas, Natural–Geology–
Montana–Bearpaw Mountains region. I. Title. II. Series. III. Series:
Geological Survey Bulletin 1521.
QE75.B9 no. 1521 [QE471.15.S25] 557.3s 81-607963 [552'.5] AACR2

For sale by the Superintendent of Documents, U.S. Government Printing Office
Washington, D.C. 20402

CONTENTS

ILLUSTRATIONS

TABLES

INVESTIGATIONS OF SHALLOW GAS RESERVOIRS IN THE NORTHERN GREAT PLAINS

PETROLOGY OF THE EAGLE SANDSTONE, BEARPAW MOUNTAINS AREA, NORTH-CENTRAL MONTANA

By DONALD L. GAUTIER

ABSTRACT

The Eagle Sandstone, in the Bearpaw Mountains area of Montana, is an important conventional reservoir for shallow gas. It represents shoreline sedimentation during a major regression of the Late Cretaceous sea. Hydrocarbons in the Eagle Sandstone mainly are isotopically light methane, which was probably generated in associated source rocks early in their burial history.

The formation is composed of sandstone and lesser amounts of mudstone. The mudstones are of several varieties and contain large amounts of highly expansible mixed-layer clay and coarser grained minerals similar to those of the associated sandstones. Quartz of diverse origins makes up 30 to 50 percent of the sandstone; intermediate plagioclase (An_{30}–An_{40}), as much as 25 percent; K-feldspars, 5 to 10 percent; sedimentary, metasedimentary, and volcanic rock fragments, 10 to 30 percent; and transported dolomite grains, 5 to 10 percent. Glauconite is common, as are small amounts of biotite, muscovite, and detrital chlorite. Accessory heavy minerals are mainly apatite, zircon, garnet, tourmaline, and opaque grains. The source area for the Eagle Sandstone lay to the west and was a mixed terrane of Proterozoic Belt Supergroup metasediments, Paleozoic sedimentary rocks, and volcanic rocks of probable Cretaceous age.

Clay mineralogy, carbon isotopes in gases, vitrinite reflectance, and stratigraphic reconstruction indicate the rocks have never been buried deeper than about 1,400 m and have not undergone thermal conditions sufficient for oil generation. Diagenesis was important in determining the reservoir properties of the Eagle Sandstone. Localized calcite precipitation began shortly after deposition. Compaction and minor quartz cementation occurred as burial depths increased. Then, extensive precipitation of sparry calcite tightly sealed intergranular pores and selectively replaced plagioclase. This calcite contains isotopically light ($\delta^{13}C = -7.5$ permil) carbon. Siderite developed locally, usually because of increased iron activities associated with altering biotite. Dissolution of calcite cement and especially dissolution of calcite replacements of plagioclase significantly enhanced reservoir porosity. These processes provided space for precipitation of authigenic clays. The present distribution of calcite-cemented layers limits vertical permeability and compartmentalizes the reser-

voirs. Early-formed carbonates may have acted as gas-trapping seals, particularly in lower permeability reservoirs to the east. Fluid-sensitive authigenic clays and iron carbonates may cause formation damage if not taken into account during the development of gas recovery methods. The Eagle Sandstone displays many diagenetic features similar to those of rocks that have undergone thermal maturation sufficient for the generation of oil or gas. It is concluded that thermal maturation of organic matter is not required for the development of significant secondary porosity, nor for the occurrence of a complex diagenetic history.

INTRODUCTION

The Bearpaw Mountains, located in north-central Montana, constitute a complex physiographic feature, which includes a central northeast-trending composite anticlinal uplift (the Bearpaw Mountains arch) flanked by volcanic rocks of Eocene age (fig. 1). Numerous shallow intrusives occur in the area, and pre-volcanic sedimentary rocks are present in downfaulted blocks within and adjacent to the volcanic fields. The Eagle Sandstone in this vicinity is an important conventional reservoir for natural gas. Low-permeability facies of the Eagle Sandstone in Canada, which are included in the Milk River Formation, are prolific producers of natural gas. Similar rocks in eastern Montana are potentially important low-permeability reservoirs. Stratigraphic studies of the Eagle in the area (Rice, 1980), isotopic investigations of gases from the Eagle Sandstone at Tiger Ridge field in the Bearpaw Mountains (Rice, 1975), vitrinite reflectance of coal by N. H. Bostick (written commun., 1979), and clay mineral data reported herein all indicate that the Eagle Sandstone has never been subjected to burial depths great enough to produce the degree of thermal maturation of source rocks required for the generation of liquid hydrocarbons (oil). Burial depth has also been insufficient to cause major phyllosilicate transformations due to burial diagenesis. Nevertheless, postdepositional chemical and biological processes have played a significant role in developing both the reservoir properties of the Eagle Sandstone and the methane-rich natural gas entrapped within it.

This report summarizes the results of a petrologic examination of four cores from productive gas wells in the Eagle Sandstone of the Bearpaw Mountains area. The purposes of this paper are to (1) describe this important conventional shallow methane reservoir, (2) develop a framework upon which to base related petrologic studies of low-permeability gas reservoirs to the east, and (3) discuss the extent

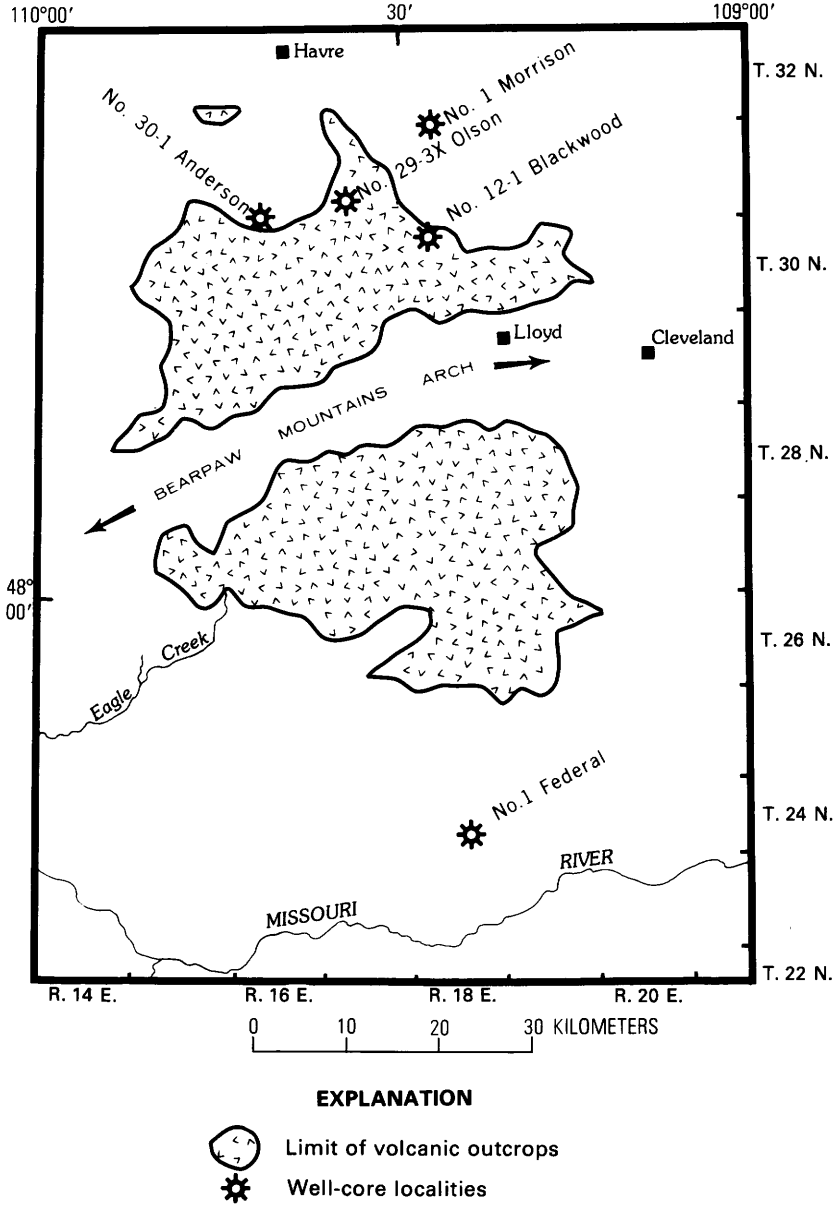

FIGURE 1.—Index map of Bearpaw Mountains study area, Montana, showing well-core localities.

to which postdepositional processes have controlled the reservoir properties of a sandstone that has not been subjected to significant burial depths.

PROCEDURE

Samples were collected from five cores of producing wells in the Eagle Sandstone. Specimens from four of these cores are considered in detail in this paper; their names and locations are listed in table 1. The fifth core (High Crest Oils No. 12-1 Blackwood) is only discussed briefly, as it displays somewhat anomalous petrologic properties, some of which have been described previously (Gautier, 1979).

Two thin sections were made from each of 170 samples. One of these was impregnated with a clear plastic resin and stained for plagioclase and potassium feldspar, and the duplicate was impregnated with a blue-dyed epoxy to facilitate observations of porosity distribution. One half of each color-impregnated slide was stained with Alizarin Red, for the determination of $CaCO_3$. Petrographic point counts of mineral composition were made for most pairs (500 points on each thin section), and detailed petrographic examinations of these samples were used to determine textural and paragenetic relationships. Heavy mineral separates from 10 sandstones were examined petrographically. Approximately 40 samples of sandstone and mudstones were subjected to bulk X-ray diffraction

TABLE 1.—*Locations and descriptions of sampled cores of Eagle Sandstone from the Bearpaw Mountains area, Montana*

Well name	Location	Cored interval (meters)	Producing interval (meters)
High Crest Oils No. 30-1 Anderson.	NE 1/4 SW 1/4 sec. 30, T. 31 N., R. 16 E.	420-446	Most of core.
High Crest Oils No. 29-3X Olson.	SE 1/4 NW 1/4 sec. 29, T. 31 N., R. 17 E.	511-557	490-546
High Crest Oils No. 1 Morrison.	NW 1/4 SE 1/4 sec. 6, T. 31 N., R. 18 E.	393-402	390-399
High Crest Oils No. 12-1 Blackwood.	NE 1/4 NW 1/4 sec. 12, T. 30 N., R. 17 E.	383-418	383-390
Fuelco No. 1 Federal 26-24-18-B.	SW 1/4 NW 1/4 sec. 26, T. 24 N., R. 18 E.	424-429 429-436	432-434

analysis, and clay-size ($< 4\mu m$) separates were made from each of these. Clay mineral identifications were made from diffractograms of oriented material mounted on porous unglazed porcelain tiles. Each oriented mount was scanned from 2° to 38° two-theta after each of four treatments: (1) air-dried but otherwise untreated, (2) solvated with ethylene glycol vapor, (3) heated to 400°C, and (4) heated to 550°C. The approximate abundances of various clays were estimated according to the method of Schultz (1964, 1978) and reported in percent. However, these values are included for comparative purposes only. Other specific mineral identifications also employed X-ray diffraction. Detailed observations of pore textures and paragenesis for 40 samples of sandstone were made with a scanning electron microscope (SEM). Stable carbon isotope content is reported for ten authigenic carbonates from sandstones: two of siderite cement, seven of calcite cement, and one from a calcite concretion. The determinations were made from CO_2 generated by the digestion of the carbonates with hydrochloric or phosphoric acid and analyzed with a Neir-McKinney double collecting mass spectrometer. Grain-size analyses of coarse silt and sand fractions were performed on an IMANCO electronic image analyzer[1], while the relative abundance of allogenic clays in mudstones was estimated by means of petrographic point counts.

This investigation focused upon sandstone lithologies, as the dominant interest of the study was the gas-bearing reservoirs of the Bearpaw Mountains. However, mudstone lithologies are also briefly described, with particular emphasis on their clay-mineral content. Most of the diagrams and many of the photomicrographs included in this report refer to the 30–1 Anderson well, located in sec. 30, T. 31 N., R. 16 E. (fig. 1). This emphasis is for illustrative purposes only, as most samples from all the cores display similar petrologic properties. Where significant differences exist, they are noted in the text and illustrated appropriately.

ACKNOWLEDGMENTS

Appreciation is expressed to personnel of the U.S. Geological Survey who provided technical assistance during the course of this investigation. Stratigraphic information, gas isotope data, and many helpful discussions were provided by Dudley D. Rice. Access to the mass spectrometer was obtained by George E. Claypool. Charles N.

[1] Use of brand names in this report is for descriptive purpose only and does not constitute endorsement by the U.S. Geological Survey.

Threlkeld prepared carbonate samples and analyzed them using the mass spectrometer. Pamela J. Ellerman made sample preparations and operated the X-ray diffractometer. Thin sections were prepared by Kenneth L. Gardner. Michael B. Sawyer provided access to the image analyzer and assisted in its operation.

GEOLOGIC SETTING

The Upper Cretaceous rocks of the northern Great Plains consist of eastward-thinning wedges of regressive sediments, which intertongue with westward-thinning transgressive deposits. The Eagle Sandstone in the vicinity of the Bearpaw Mountains represents shoreline sedimentation which culminated the Telegraph Creek-Eagle regression, the second of four major Late Cretaceous regressions recognized in the northern Great Plains. This retreat of the epicontinental sea began as early as 85 m.y. ago during the time of the ammonite *Scaphites depressus* (Gill and Cobban, 1973, p. 20). The regression was accompanied, in west-central Montana, by the formation of the lower portion of the Elkhorn Mountains Volcanics. In north-central Montana, this episode is represented by the upward transition of the Niobrara Formation into the Telegraph Creek Formation, which, in turn, is conformably overlain by shoreline deposits of the Eagle Sandstone.

In the Bearpaw Mountains area, the Eagle Sandstone was probably deposited under conditions similar to those described from subsurface and outcrop studies to the south by Rice (1980). It generally consists of three members (fig. 2): (1) The basal Virgelle Sandstone Member, poorly developed in boreholes of this study, which is dominated by sandstone deposited along a prograding coastal, interdeltaic shoreline; (2) a regionally variable, unnamed middle member, consisting of sandstones, siltstones, mudstones, shales, and minor impure lignite deposited in a coastal plain and deltaic setting; and (3) a disconformably overlying, unnamed upper member containing sandstone, siltstone, and shale primarily accumulated on a tidal flat or beachface.

Deposition of the Eagle Sandstone was terminated abruptly by the rapid advance of the Claggett sea. This transgression began with subsidence and explosive volcanism, recorded by the Ardmore Bentonite Beds, and corresponds with the lowest part of the faunal zone

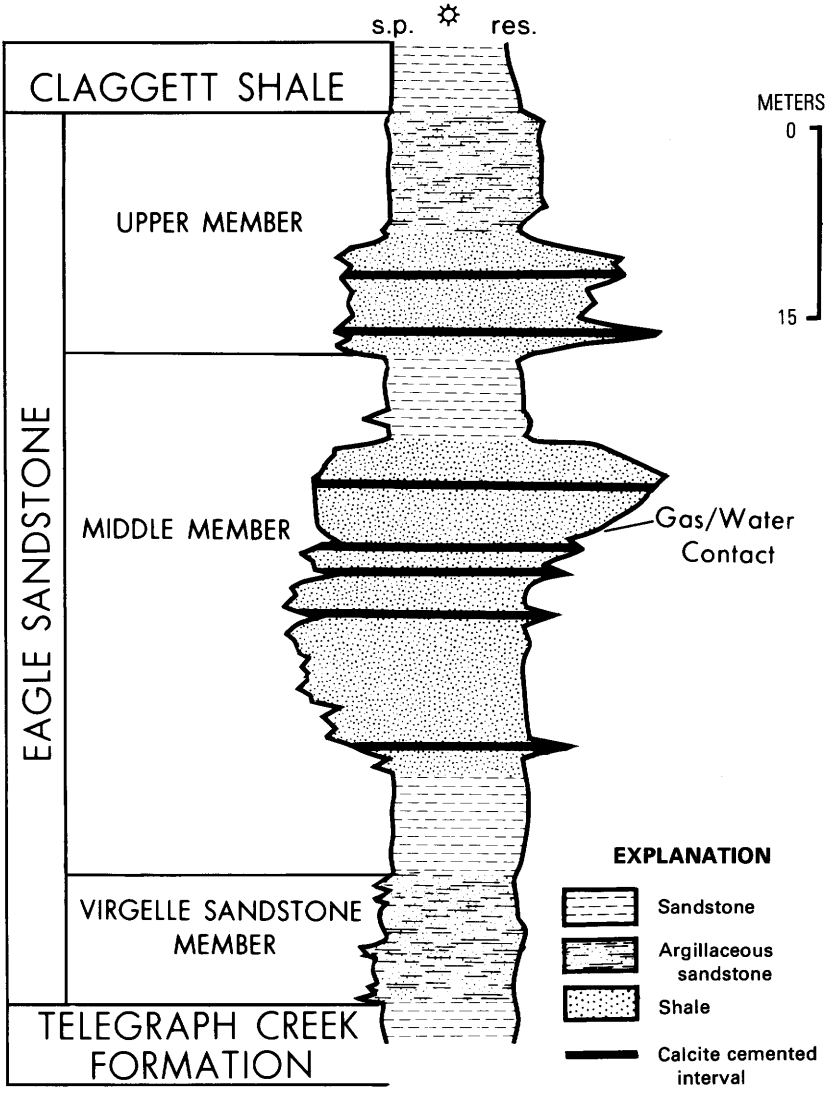

FIGURE 2.—Lithologies and resistivity (res.) and spontaneous potential (s.p.) log response for the 30-1 Anderson well.

of *Baculites obtusus* (Gill and Cobban, 1973, p. 20), approximately dated at 79 m.y. (Obradovich and Cobban, 1975, p. 36). In many places, the uppermost portion of the Eagle Sandstone and the lowermost part of the overlying Claggett Shale contain conglomeratic laminations of chert pebbles, possibly representing a lag deposit associated with this transgression.

In the vicinity of the Bearpaw Mountains, the Eagle Sandstone was subsequently buried beneath marine and continental rocks of Late Cretaceous and early Tertiary age. These sediments, consisting of the Claggett Shale, the Judith River Formation, the Bearpaw Shale, the Fox Hills Sandstone, the Hell Creek Formation, and the Fort Union Formation, accumulated to thicknesses that probably average 1,220 to 1,370 m (D. D. Rice, oral commun., 1979) and do not exceed a maximum of 1,650 m in any location (Hearn, 1976).

The onset of intrusion, uplift, and volcanism in late early Eocene or middle Eocene time terminated deposition in the Bearpaw Mountains area and initiated the major features of the modern Bearpaw Mountains anticlinal structure. Recent work by Hearn (1976), in general agreement with Maher (1969), has vindicated the interpretation made long ago by Reeves (1924, 1946) that this complex structure resulted from gravity sliding of sedimentary rocks, including the Eagle Sandstone, and overlying volcanics along gently dipping planes in the Colorado Shale. This sliding apparently occurred during or between episodes of volcanism, because older extrusives are involved in the structure to a much greater extent than younger ones, which may overlie both tilted sedimentary rocks and older volcanic rocks.

HYDROCARBONS IN THE EAGLE SANDSTONE

Large quantities of natural gas are present at shallow depths in the Bearpaw Mountains area. Schorning (1972, p. 153) estimated the proven reserves in the northern part of the field alone to be about 20.8 billion cubic meters. This gas occurs as accumulations entrapped in the heads of gravity-slide blocks on the flanks of the Bearpaw Mountains anticlinal structure. Chemical and isotopic studies by Rice (1975) indicate that the gas is composed of more than 99 percent methane enriched in the light isotope C^{12}, with $\delta^{13}C$ values ranging between -66 and -70 permil, relative to the PDB Chicago standard. These values strongly suggest that the gas was formed through the reduction of CO_2 or HCO_3^- by methane-generating bacteria (Rice, 1975) under conditions analogous to those outlined by Claypool and Kaplan (1974) for marine sediments examined during the Deep Sea Drilling Project.

If the natural gas in the Bearpaw Mountains area was generated by a process similar to that observed in recent marine sediments, the methane must have formed early in the burial history of the rocks. Gas was probably produced prior to complete expulsion of interstitial water, by anaerobic bacteria. The bacteria acted upon the abundant organic matter contained in sediments associated with the Eagle Sandstone, such as the Niobrara Formation or the Claggett Shale. Progressive compaction injected both methane and interstitial bicarbonate-rich waters into the sandstone. Coals within the Eagle Sandstone, in this area, are volumetrically insignificant and could not have served as an important source of organic material for this process.

LITHOLOGY

The Eagle Sandstone may be divided into two broad lithologic categories. Most of the formation is a medium-gray (N5), well-sorted, angular, fine-grained sandstone. This lithology is generally highly porous (25 percent) and permeable (100–300 md), and it forms conventional gas reservoirs of the type now being explored for in the Bearpaw Mountains area. The second general lithologic category used in this report is termed mudstone. Characteristic lithologies and associated electric log responses for the 30–1 Anderson well are illustrated in figure 2.

MUDSTONES

Mudstones, as used in this report, comprise a diverse assemblage of lithologic types, including shales, siltstones, argillaceous sandstones, and rare thin coals. These sediments were probably deposited under a variety of conditions and occur in both nearshore marine and continental sequences.

True shales, or silty shales, display strong phyllosilicate orientation parallel to bedding, which is commonly defined by horizontally arranged platelets and irregular masses of organic material. Strongly laminated rocks, consisting of intercalated finer and coarser lithologies, may be present and undisturbed. However, it is more common to observe disruptions in the bedding and mixing of lithologic types due to bioturbation. The effects of burrowing organisms are variable in intensity. These range from small sand-filled burrows within shaly sequences and clay-filled burrows in sandy units to completely mixed, unsorted rocks, which display no hint of their original orienta-

tion or bedding. Body fossils are essentially absent from the samples examined in this investigation, although both marine and nonmarine fossils have been reported from the Eagle Sandstone in the study area.

Silt- and sand-sized constituents of these mudstones are composed of materials similar to those that compose the reservoir sandstones with which they are associated. They differ only in their finer grain size and the resulting lower proportion of rock fragments, and in their association with abundant allogenic clay. Postdepositional effects observable in thin section are limited to pyrite, often associated with organic material, dissolution features in silicate fragments, and small patches of iron-rich carbonate scattered about the rock. SEM studies reveal similar features, except that flamelike phyllosilicates are commonly observed upon allogenic clays. These are probably authigenic. Calcite concretions are occasionally seen.

The clay-size fraction (< 4 μm) from marine and nonmarine mudstones of the Eagle Sandstone displays a consistent mineralogical composition (table 2). It contains some quartz and feldspar but otherwise consists almost entirely of phyllosilicates. In mudstones, this assemblage is dominated by mixed-layer illite-smectite with lesser amounts of clay-size mica, kaolinite, and chlorite of undetermined composition. The mixed-layer mineral is randomly ordered and contains from 10 to 30 percent illite-like layers and 70 to 90 percent smectitic layers. This composition is similar to that reported by Schultz and others (1980) for clay minerals of continental and marine rocks of the Pierre Shale and its equivalents, which include, among others, the Eagle Sandstone and its westward continental equivalent, the Two Medicine Formation. They interpret most of the highly expansible mixed-layer illite-smectite as being volcanogenic. They further suggest that the similarity between marine and nonmarine clays, also observed in the present study, is probably indicative of a detrital origin for most of these minerals. I concur with these views.

Convincing investigations of depth-related mineral transformations within mixed-layer illite-smectites in pelitic sediments of the Gulf Coast have been conducted by Powers (1959), Burst (1959), Weaver (1960), Perry and Hower (1970), Hower and others (1976), Aronson and Hower (1976), and many others. This work has demonstrated that, in the Gulf Coast area, highly expansible mixed-layer minerals undergo a temperature-controlled burial diagenesis which converts smectitic layers to illite-like layers at depths between 1,525 m and approximately 4,575 m. Mixed-layer clays containing 80 percent or more expanding layers were found to persist to depths of about 1,525 m. Beyond this, they become more illitic, until at depths of about 4,575 m no more than 20 percent expansible layers

TABLE 2.—*Clay mineral data for selected samples of Eagle Sandstone*

[Data in percent]

Depth (m)	Lithology	Kaolinite	Mica	Chlorite	Mixed-layer clay	
					Abundance	Percent expansible[1]
		30-1 Anderson Core				
420.3	Sandstone----	68	20	2	10	N
420.3	Sandy marine shale------	28	19	4	49	70
420.6	Sandstone----	68	10	1	21	80
421.2	----do-------	66	10	1	23	N
422.1	----do-------	59	11	2	28	80
425.2	Nonmarine mudstone---	10	12	3	75	80
426.4	----do-------	20	20	3	57	90
426.4	----do-------	13	26	5	56	70
426.4	----do-------	32	21	2	45	70
427.3	----do-------	19	30	4	47	80
427.9	----do-------	13	15	3	69	90
428.5	----do-------	36	18	2	44	80
429.2	----do-------	13	22	3	62	70
430.7	Sandstone----	87	3	2	8	70
431.3	----do-------	88	6	0	6	N
431.9	----do-------	82	9	1	8	80
438.0	----do-------	86	5	2	7	N
443.5	----do-------	79	8	3	10	N
445.3	----do-------	85	6	2	7	N
		1-Morrison Core				
393.2	Sandstone----	85	6	2	7	N
399.6	----do-------	67	13	1	19	N
401.4	----do-------	75	12	3	10	N
		29-3X Olson Core				
510.8	Marine mudstone---	38	40	10	12	80
515.1	Sandstone----	70	24	1	5	N
518.2	Argillaceous sandstone.	52	22	2	24	80
524.6	Shale--------	18	21	3	58	80
527.6	Sandstone----	75	7	1	17	N
534.0	----do-------	85	6	1	8	N
541.3	----do-------	82	12	1	5	N
546.2	----do-------	74	8	1	17	70
550.2	Argillaceous sandstone.	61	11	1	27	85
554.7	Marine(?) mudstone	24	24	3	49	85

[1] N=No determination.

remain. A similar process has been proposed to explain the presence, within rocks of the Montana disturbed belt, of mixed-layer clays that display a regular alteration of illitic and smectitic layers (IS ordering) and contain less than 40 percent expanding layers (Hower and Hall, 1970; Hoffman, 1976; Hoffman and others, 1976; Hoffman and Hower, 1979), because Cretaceous argillaceous sediments in this disturbed belt have been buried to great depths under thrust sheets. However, work by Schultz (1978) seems to indicate that burial diagenesis will not fully explain mineralogical variation within mixed-layer minerals of the Pierre Shale in other areas of the northern Great Plains.

While a large percentage of illite-like layers within a mixed-layer clay may not demonstrate that burial diagenesis has occurred (Schultz, 1978), it is likely that a predominant content (> 80 percent) of expansible layers indicates that such alterations have not developed and that temperatures required for the thermocatylitic generation of oil from organic matter have never been attained (Burst, 1959). The preponderance of expansible layers within mixed-layer

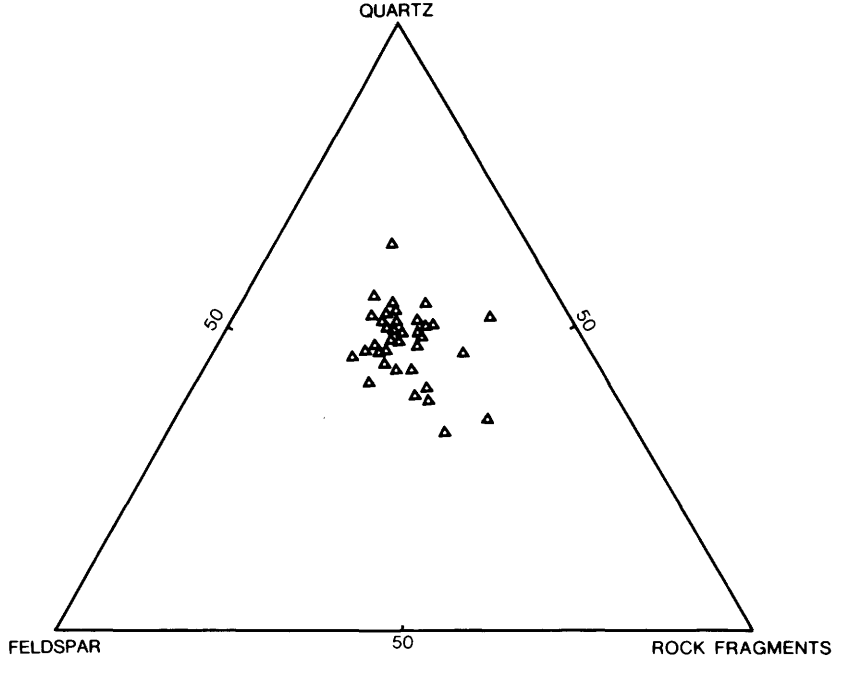

FIGURE 3.—Typical quartz, feldspar, and rock-fragment proportions of the Eagle Sandstone.

clays of marine and nonmarine mudstones is considered strong evidence that no significant temperature-controlled clay-mineral transformations have occurred within the Eagle Sandstone in the vicinity of the Bearpaw Mountains. This interpretation is consistent with reconstructed burial depths and with vitrinite reflectance values in oil (R_0) of 0.4 for coal from the 30-1 Anderson well (N. H. Bostick, written commun., 1979), which are well below those required for oil generation (Bostick, 1979, p. 28-29). All of these factors are consistent with the biogenic origin of the methane-rich gas at Tiger Ridge Field.

SANDSTONE FRAMEWORK

The majority of the Eagle Sandstone is composed of sandstone containing little or no allogenic clay. Although Rice (1980) has demonstrated that these rocks may have accumulated in a variety of environments, the petrologic consistency of their framework grain composition, grain size, and post-depositional history clearly warrants that they be considered as a group. This section describes detrital components of the sandstones, including quartz, feldspars, lithic fragments, varietal constituents, and accessory heavy minerals. Framework grain compositions, excluding dolomite, for typical sandstones are illustrated in figure 3; petrographic data are listed for many typical sandstones in table 3; variations of composition as a function of depth and lithology are shown in figure 4; typical grain-size distributions for silt and sand components of the 30-1 Anderson core are displayed in figure 5; and relative abundances of framework grains, allogenic clay, carbonate cement, and pore space are shown in figure 6 and listed in table 4.

QUARTZ

Quartz grains are generally the most abundant single component of the sandstone framework, typically constituting 30 to 50 percent of the rock. These grains are dominantly monocrystalline (table 5). Most of the monocrystalline grains display straight or slightly undulatory extinction, irregular grain boundaries, and inclusions, some of which are organized in "bubble trains." Some (10-20 percent) irregular quartz fragments show strongly undulatory extinction, numerous inclusions, and may have a "stretched" appearance. At least some of these fragments can be attributed to a metamorphic source. Virtually every sample contains a small quantity of quartz grains interpreted to be of volcanic origin. These grains commonly display the bipyramidal habit of beta quartz and always occur as euhedral, rounded euhedral, or fragmented euhedral crystals with absolutely straight

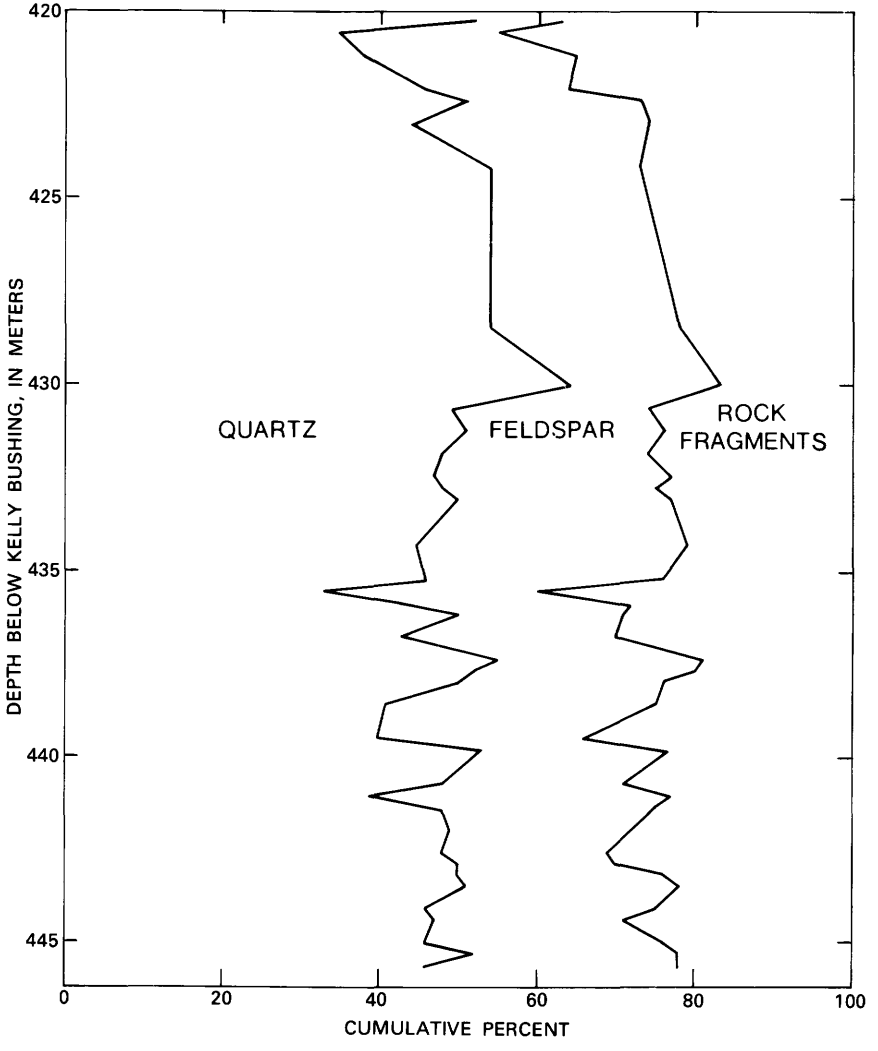

FIGURE 4.—Proportional variations in quartz, feldspar, and rock-fragment content with depth in the 30-1 Anderson core.

extinction and very few inclusions other than rare isotropic glass (fig. 7*A*). Many of these volcanogenic fragments have resorbed boundaries and may be attached to remnants of isotropic or slighty birefringent groundmass material. These grains were once phenocrysts in an extrusive or shallow intrusive igneous rock of siliceous

TABLE 3.—*Petrographic data for selected thin sections of the Eagle Sandstone from the Bearpaw Mountains, Montana*

[Abundances in percent, N, not determined]

Depth (m)	Quartz (excluding chert)	Chert	Feldspar			Rock fragments	Biotite	Glauconite	Muscovite	Dolomite grains	Calcite cement	Iron carbonate	Authigenic clay	Clay matrix	Total	Average quartz size (mm)
			Plagioclase	K-feldspar	Total											
30-1 Anderson core																
420.3	42	13	6	3	9	16	1	5	0	2	0	<1	<1	11	99	N
420.6	43	4	6	7	13	32	6	1	0	0	0	0	<1	<1	99	0.09
421.2	26	3	7	9	16	26	2	1	<1	6	19	1	<1	0	100	.09
422.1	29	1	6	5	11	16	1	<1	0	9	31	2	<1	0	100	.1
422.5	40	6	9	8	17	15	2	<1	0	6	9	2	1	0	98	.12
423.1	34	5	12	11	23	15	1	1	1	16	0	3	<1	<1	99	.09
424.3	22	1	5	3	8	10	<1	1	0	3	0	1	<1	53	99	.09
428.5	9	<1	N	N	4	3	<1	0	<1	6	0	<1	<1	77	99	.07
430.1	42	6	7	5	12	5	0	0	0	3	0	1	<1	31	100	N
430.7	42	8	15	6	21	14	0	0	0	<1	0	<1	<1	15	100	.15
431.3	51	4	18	6	24	19	0	<1	<1	1	0	<1	<1	0	99	.2
431.9	47	9	20	6	26	17	<1	<1	0	<1	<1	<1	1	0	100	.27
432.5	45	9	19	10	29	13	1	<1	<1	<1	<1	<1	2	0	99	.22
432.8	47	9	18	8	26	16	1	0	0	<1	<1	<1	1	0	100	.19
433.1	48	9	20	7	27	14	1	<1	0	<1	<1	<1	<1	0	99	.22
434.3	43	7	22	10	32	13	1	1	0	0	<1	<1	2	0	99	.19
435.3	31	8	11	9	20	8	2	0	0	0	30	0	<1	0	99	N
435.8	39	13	15	15	30	16	1	1	0	0	<1	<1	<1	0	100	N
436.2	49	11	12	8	20	17	2	0	0	0	0	<1	<1	0	99	N
436.7	41	14	20	6	26	16	3	0	<1	0	0	<1	<1	0	100	N
437.4	55	9	20	5	25	9	1	<1	0	0	<1	0	<1	0	98	N
437.7	52	6	22	6	28	14	0	0	0	0	<1	0	<1	0	100	.16
438.0	48	10	16	9	25	14	<1	<1	0	0	<1	<1	1	0	98	N
438.5	40	8	20	13	33	17	2	0	0	<1	<1	0	<1	0	100	.19
439.5	35	4	14	8	22	26	1	<1	<1	2	9	1	<1	0	100	.16
440.0	35	2	11	5	16	13	0	<1	0	2	30	<1	<1	<1	98	.22
440.5	44	5	18	4	22	22	<1	1	0	3	<1	<1	<1	0	97	.16
441.0	45	2	18	7	25	22	<1	0	0	4	<1	2	<1	0	100	.16
442.0	45	2	14	6	20	25	1	<1	0	4	2	1	<1	0	100	.16
442.5	45	2	15	5	20	27	<1	<1	0	4	<1	<1	<1	0	98	.16
442.9	41	3	12	5	17	22	1	1	0	5	10	<1	<1	0	100	.16
443.2	34	2	11	7	18	15	0	<1	0	4	30	<1	<1	<1	103	N
443.5	47	3	18	7	25	18	<1	<1	<1	4	<1	1	<1	0	98	.13
444.1	41	4	16	9	25	18	<1	1	Tr	<1	0	<1	<1	0	89	.13
444.4	45	4	15	6	21	23	<1	<1	0	5	0	1	<1	0	99	.15
445.0	42	3	19	8	27	18	>1	<1	0	7	0	<1	<1	0	97	.16
445.3	49	3	20	5	25	18	0	0	0	4	0	<1	<1	0	99	.18
445.6	42	4	21	8	29	16	2	<1	0	4	0	<1	1	0	98	.16

TABLE 3.—*Petrographic data for selected thin sections of the Eagle Sandstone from the Bearpaw Mountains, Montana*—Continued

Depth (m)	Quartz (excluding chert)	Chert	Feldspar			Rock fragments	Biotite	Glauconite	Muscovite	Dolomite grains	Calcite cement	Iron carbonate	Authigenic clay	Clay matrix	Total	Average quartz size (mm)
			Plagioclase	K-feldspar	Total											
Fuelco No. 1 Federal core																
425.0	28	8	10	6	16	5	2	3	<1	2	35	1	<1	0	100	N
425.7	30	6	3	4	7	13	2	1	1	5	<1	1	<1	33	99	N
425.8	33	12	2	4	6	14	<1	1	1	N	N	N	<1	28	95	.07
426.6	34	19	1	6	7	9	<1	3	0	0	24	2	<1	2	100	N
426.9	48	18	4	5	9	18	<1	<1	<1	<1	<1	<1	<1	4	97	.16
427.5	36	15	2	8	10	19	<1	4	0	5	<1	5	<1	6	100	N
430.8	34	10	0	6	6	11	<1	7	<1	0	0	<1	<1	31	99	.11
431.1	42	16	1	7	8	15	<1	3	<1	0	0	<1	<1	16	100	.12
431.4	35	14	0	7	7	7	0	3	0	0	25	<1	<1	7	98	N
433.6	54	14	5	7	12	15	<1	3	0	<1	0	<1	<1	0	98	.12
433.9	46	13	5	10	15	20	<1	3	0	<1	0	<1	<1	0	97	N
434.2	39	10	1	3	4	9	1	4	<1	<1	0	9	<1	20	96	N
434.8	35	11	3	8	11	28	2	5	0	2	0	3	<1	2	99	N
435.1	54	16	<1	4	4	16	<1	2	0	<1	0	<1	<1	6	98	N
435.4	21	5	2	2	4	8	0	<1	0	<1	0	0	<1	60	98	N
No. 1 Morrison core																
393.2	47	7	7	6	13	26	<1	6	<1	0	<1	0	<1	0	99	.18
393.8	49	6	7	3	10	30	1	3	0	0	0	<1	<1	0	99	.22
394.4	51	5	11	6	17	25	<1	1	0	0	0	0	<1	0	99	N
395.6	55	7	5	7	12	24	0	1	0	0	<1	0	<1	0	98	N
396.2	48	9	2	5	7	26	<1	6	0	0	0	0	2	0	98	.28
396.8	44	9	4	7	11	31	<1	2	0	0	0	0	<1	0	97	N
397.4	51	9	7	6	13	21	<1	4	0	0	0	0	2	0	100	.25
397.8	55	7	7	5	12	23	0	3	0	0	0	0	<1	0	100	N
398.4	52	8	5	6	11	25	<1	3	0	0	0	0	1	0	100	.22
399.0	55	8	7	2	9	23	0	4	0	0	0	0	1	0	100	N
399.6	45	9	6	7	13	25	<1	7	0	0	0	0	1	0	100	.25
400.2	56	5	4	4	8	27	0	3	0	0	0	0	<1	0	99	N
400.8	52	6	6	7	13	22	0	6	0	0	<1	0	1	0	100	N
401.4	50	6	11	6	17	22	<1	4	0	0	0	0	<1	0	99	N
401.7	45	14	8	5	13	24	<1	1	<1	0	<1	0	2	0	98	.25

composition. Polycrystalline fragments are also common and may form as much as 34 percent of all quartz in a particular sample. These grains are of diverse origin; some appear to be simply very coarse quartz chert, while others can be identified as fragments of quartzose siltstone, metasiltstone, or fine-grained quartzarenite. Many other polycrystalline quartz grains cannot be confidently attributed to any specific source.

TABLE 3.—*Petrographic data for selected thin sections of the Eagle Sandstone from the Bearpaw Mountains, Montana*—Continued

Depth (m)	Quartz (excluding chert)	Chert	Feldspar			Rock fragments	Biotite	Glauconite	Muscovite	Dolomite grains	Calcite cement	Iron carbonate	Authigenic clay	Clay matrix	Total	Average quartz size (mm)
			Plagioclase	K-feldspar	Total											
No. 29-3X Olson core																
516.0	46	10	4	7	11	14	0	3	0	2	4	7	<1	N	97	N
518.2	46	11	7	4	11	12	1	3	0	<1	<1	12	<1	N	96	N
519.4	43	9	4	2	6	24	<1	2	0	7	0	<1	3	N	94	N
520.3	42	8	1	6	7	21	1	3	0	10	<1	1	2	N	95	N
521.5	53	8	3	2	5	17	0	1	0	4	0	2	<1	N	90	N
No. 29-3X Olson core--Continued																
522.4	44	3	6	2	8	22	<1	1	0	9	<1	8	<1	N	95	N
523.6	48	5	7	2	9	18	<1	1	0	11	3	1	1	2	99	N
527.6	32	4	7	4	11	13	<1	0	0	2	36	1	<1	0	99	N
528.2	32	3	5	5	10	7	1	0	0	1	43	2	<1	0	99	N
529.7	55	3	11	6	17	21	2	N	N	0	2	0	<1	0	100	N
531.0	61	2	14	3	17	19	0	<1	0	0	<1	N	<1	0	99	N
532.8	44	3	22	5	27	19	0	<1	0	0	6	0	<1	0	99	N
534.0	40	17	15	9	24	15	<1	<1	0	0	2	0	<1	0	98	N
535.2	53	10	11	3	14	15	0	0	0	0	7	<1	<1	0	99	N
535.8	40	9	21	8	29	19	<1	<1	0	0	<1	0	<1	0	97	N
536.4	56	5	18	6	24	15	<1	<1	0	0	<1	0	<1	0	100	N
537.7	52	5	21	6	27	14	<1	0	0	<1	<1	<1	<1	0	98	N
538.3	37	7	14	7	21	22	0	<1	<1	7	3	<1	1	0	97	N
539.2	48	5	9	7	16	19	<1	<1	0	8	1	<1	<1	0	97	N
540.1	43	3	9	5	14	24	<1	<1	0	N	N	N	<1	0	84	N
541.3	44	6	25	5	30	14	<1	<1	0	6	0	<1	<1	0	100	N
542.2	50	4	12	6	18	20	<1	0	0	4	2	1	<1	0	99	N
543.2	43	5	14	7	21	23	<1	0	0	2	5	<1	<1	0	99	N
545.6	39	4	11	6	17	29	<1	1	0	N	N	N	<1	1	91	N
547.1	37	10	14	6	20	18	0	2	0	5	<1	5	<1	2	99	N
549.2	34	5	9	9	18	33	<1	<1	0	2	2	2	1	2	99	N
550.2	31	10	13	7	20	21	1	1	0	4	<1	6	<1	3	97	N
555.0	22	1	13	5	18	12	1	0	0	8	0	3	<1	35	100	.06

FELDSPARS

Plagioclase forms as much as 25 percent of the entire rock. The grains may be irregular, angular fragments, or lath-like crystals. Albite twinning is observed frequently, but pericline and Carlsbad twins are uncommon. Optical determinations indicate that the composition of these grains is generally no more calcic than An_{40} (andesine) in unzoned crystals. However, strong normal or oscillatory zon-

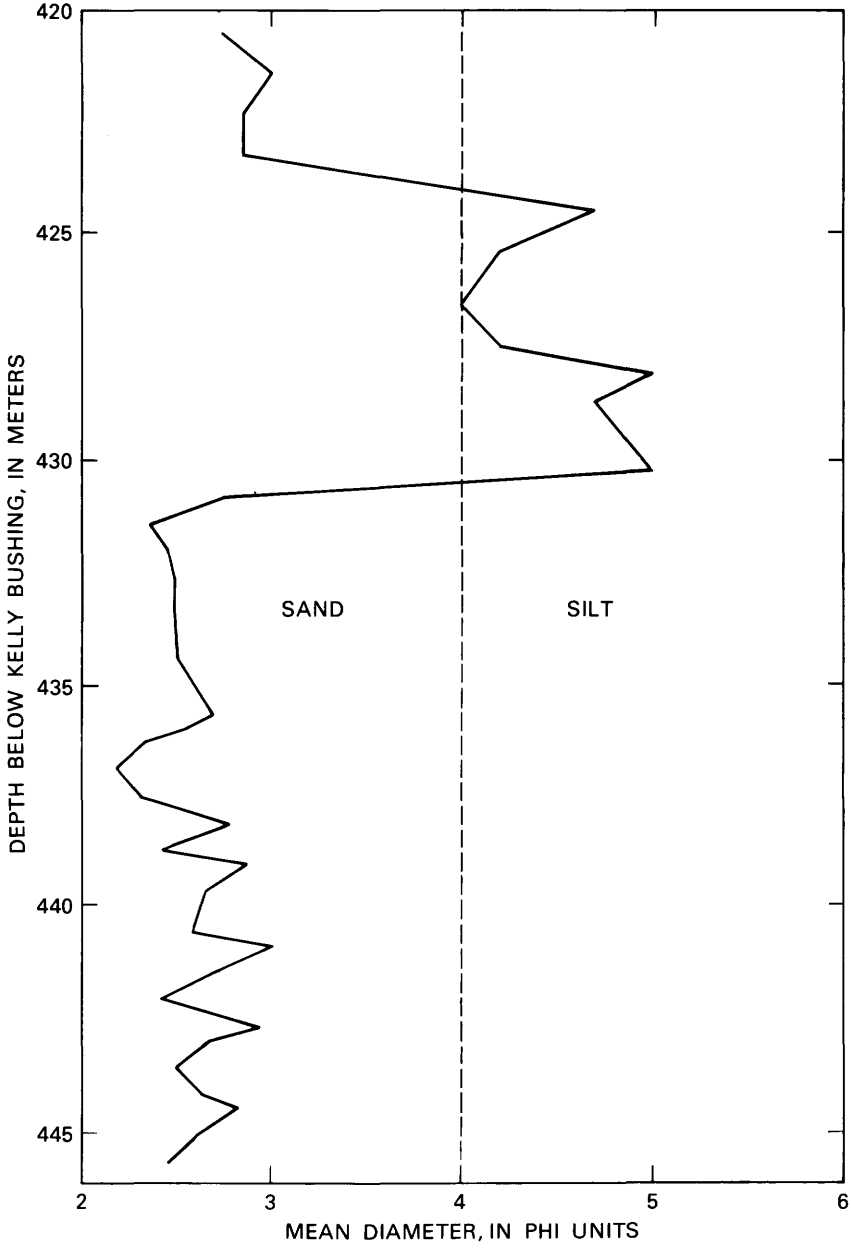

FIGURE 5.—Mean framework grain size distribution as a function of depth in the 30-1 Anderson core.

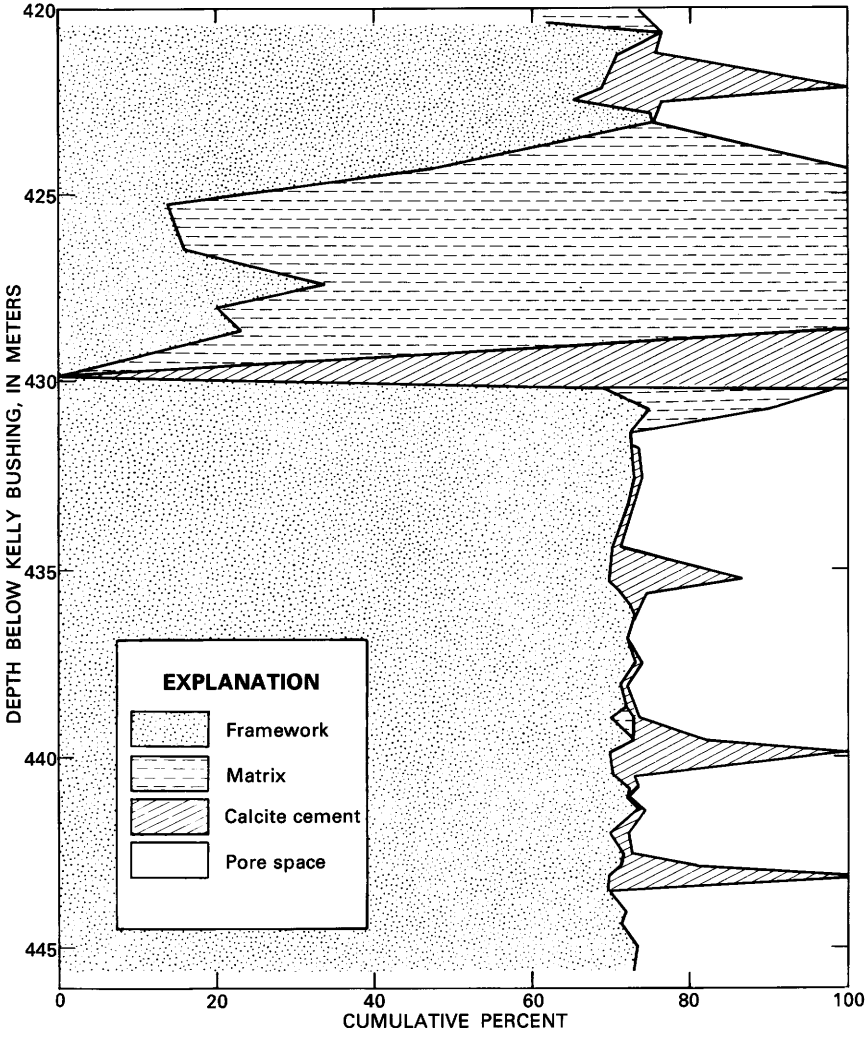

FIGURE 6.—Framework, matrix, calcite cement, and pore space (FMCP) distribution as a function of depth in the 30–1 Anderson core.

ing precludes an accurate optical determination in many cases. Rare grains that are apparently immune to conventional staining techniques but display clear, closely spaced albite twin lamellae are interpreted as albite. Plagioclase fragments are generally not affected by any sort of clay alteration. However, kaolin booklets may form indis-

TABLE 4.—*Point count data used in calculating FMCP diagram (fig. 6) for 30-1 Anderson core*

[Data in percent.]

Depth (m)	Framework	Matrix	Calcite cement	Pore space
420.3	62.1	11.0	0	26.9
420.6	76.5	0	0	23.5
421.2	71.0	0	5.0	24.0
422.1	69.0	0	31.0	0
422.5	65.4	0	11.0	23.6
422.8	74.9	0	1.0	24.1
423.1	75.3	0	0	24.7
424.3	47.0	53.0	0	0
425.2	14.0	86.0	0	0
426.4	16.0	84.0	0	0
427.3	34.0	66.0	0	0
427.9	20.0	80.0	0	0
428.5	23.0	77.0	0	0
429.8	0	0	100.0	0
430.1	69.0	31.0	0	0
430.7	75.0	25.0	0	0
431.3	72.6	0	0	27.4
431.9	72.9	0	.5	26.6
432.5	73.0	0	.5	26.5
433.1	72.3	0	.5	27.2
434.3	70.4	0	.5	29.1
435.3	70.0	0	16.0	14.0
435.6	71.5	0	2.0	26.5
435.9	72.5	0	.5	27.0
436.2	73.0	0	0	27.0
436.8	72.1	0	0	27.9
437.4	72.5	0	.5	27.0
438.0	70.9	0	.5	28.6
438.6	72.0	0	.5	27.5
438.9	70.1	3.0	0	26.9
439.5	73.1	0	9.0	17.9
439.8	70.0	0	30.0	0
440.4	70.4	0	2.0	27.6
440.7	72.4	0	.5	27.1
441.0	72.3	0	0	27.7
441.4	73.5	0	.5	26.0
442.0	70.1	0	2.0	27.9
442.6	71.8	0	.5	27.7
442.9	71.5	0	10.0	18.5
443.2	70.0	0	30.0	0
443.5	69.8	0	.5	29.7
444.1	72.1	0	0	27.9
444.4	71.6	0	0	28.4
445.0	73.4	0	0	26.6
445.6	73.0	0	0	27.0

TABLE 5.—*Quartz varieties determined by separate point counts of selected thin sections from the Bearpaw Mountains, Montana*

[Figures show number of grains]

Depth (m)	Monocrystalline		Polycrystalline	Total grains counted
	Straight extinction	Undulatory extinction		
	30-1 Anderson core			
431.3	70	62	20	152
435.3	79	17	9	105
441.0	39	58	25	122
445.3	52	69	31	152
	29-3X Olson core			
518.2	57	44	36	137
521.5	48	81	28	157
527.6	78	46	5	129
531.9	88	82	5	175
534.0	48	60	11	119
535.8	47	55	16	118
538.3	50	47	12	109
541.3	45	69	13	127
544.4	48	42	23	113
546.2	43	59	9	111
547.7	45	46	7	98
550.2	34	46	12	92

criminately upon them. Despite the absence of clay alteration, plagioclase grains are observed in various states of preservation, ranging from pristine to drastically diminished due to dissolution. Two processes are probably responsible for these effects: (1) dissolution of carbonate that had previously replaced plagioclase, and (2) dissolution of plagioclase directly by interstitial waters. These effects will be considered in a later section in more detail.

Potassium feldspars are also a volumetrically important component of the framework with abundances generally ranging between 5 and 10 percent, although they can constitute as little as 2 and as much as 15 percent of the entire rock. For this study, potassium feldspar was subdivided into three groups: complexly twinned grains (microcline), untwinned potassium feldspars with a small ($< 40°$) optic angle (sanidine), and untwinned potassium feldspars with a large ($> 40°$) optic angle (orthoclase) (table 6). Microcline is an uncommon

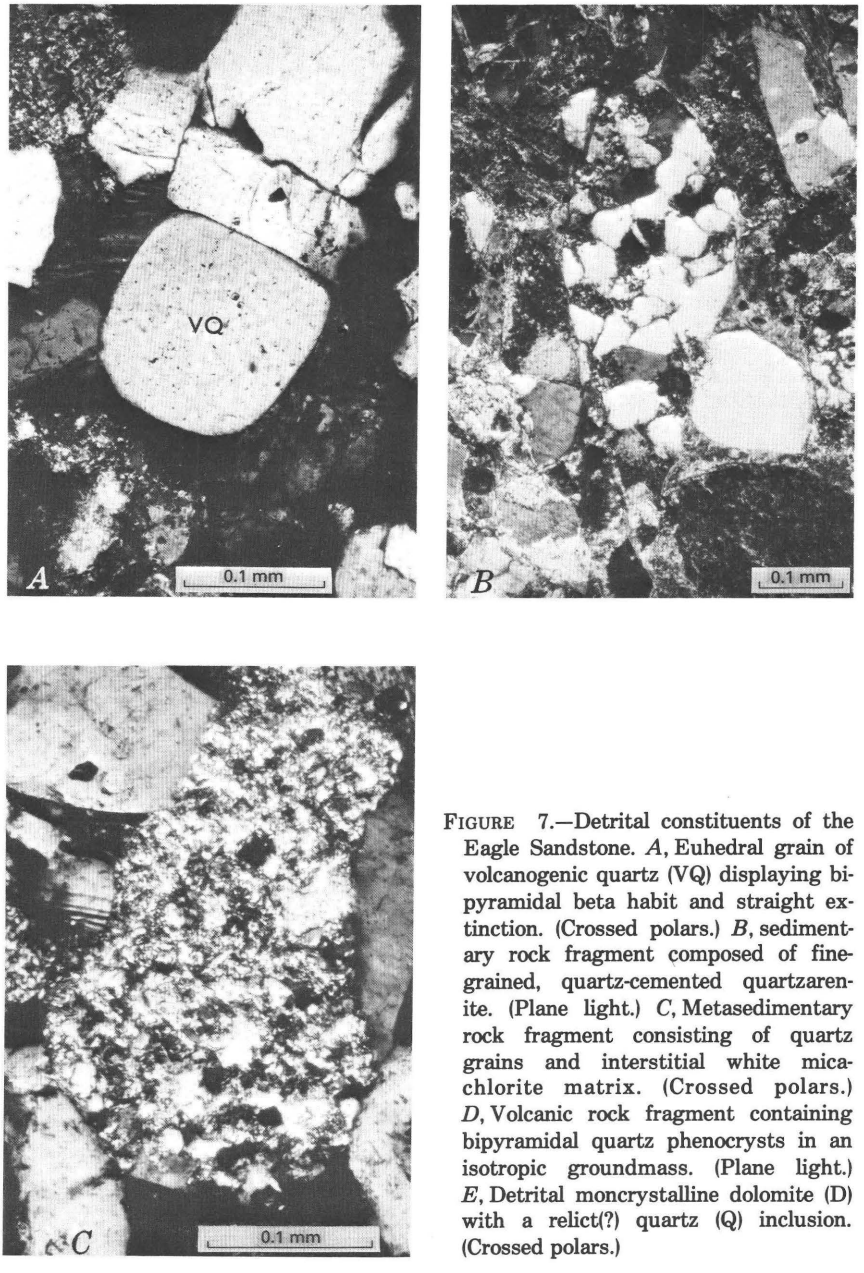

FIGURE 7.—Detrital constituents of the Eagle Sandstone. *A*, Euhedral grain of volcanogenic quartz (VQ) displaying bipyramidal beta habit and straight extinction. (Crossed polars.) *B*, sedimentary rock fragment composed of fine-grained, quartz-cemented quartzarenite. (Plane light.) *C*, Metasedimentary rock fragment consisting of quartz grains and interstitial white mica-chlorite matrix. (Crossed polars.) *D*, Volcanic rock fragment containing bipyramidal quartz phenocrysts in an isotropic groundmass. (Plane light.) *E*, Detrital moncrystalline dolomite (D) with a relict(?) quartz (Q) inclusion. (Crossed polars.)

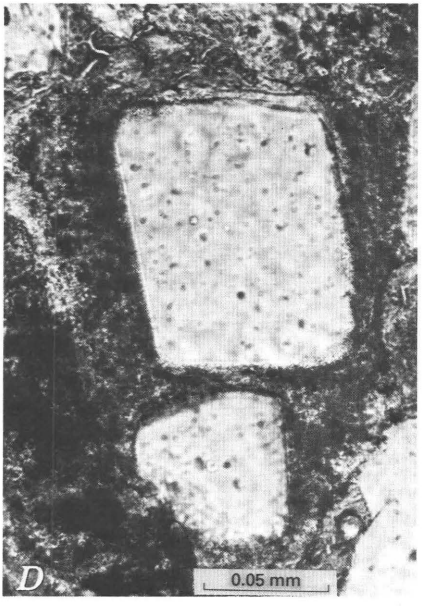

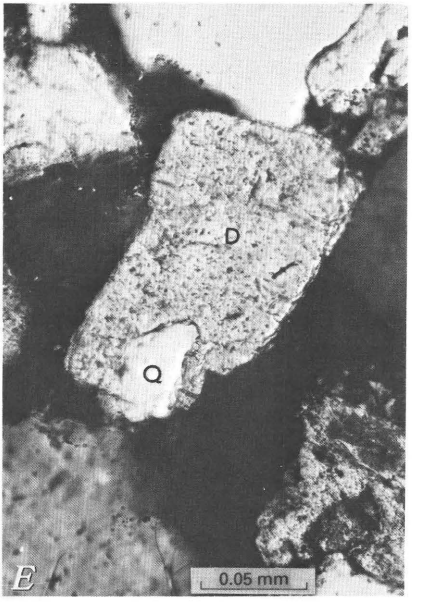

constituent with only a few grains usually present in any particular thin section. Sanidine is generally more abundant than orthoclase. Whereas many of the grains positively identified as orthoclase or microcline display irregular, angular grain boundaries, sanidine commonly possesses a subhedral to euhedral habit. In thin section, most potassium feldspars appear very fresh. However, the SEM reveals minor surficial dissolution features. Some potassium feldspars have served as a substrate for the growth of a potassium-bearing clay mineral, probably mixed-layer illite-smectite. In no case, however, were these feldspars observed to have undergone dissolution extensive enough to significantly affect rock porosity. No pseudomorphous replacement of clay for potassium feldspar was seen.

LITHIC FRAGMENTS

Rock fragments, including chert in this report, compose 10 to 30 percent of most samples (fig. 3) (table 7). These grains are of diverse origin and are found in various states of preservation. Fortu-

TABLE 6.—*Potassium feldspar content in 10 selected thin sections of the 30-1 Anderson core*

[Figures show number of grains; 2*V* is the angle between the two optic axes]

Depth (m)	Total counts	$2V > 40°$ (orthoclase)	$2V < 40°$ (sanidine)	Twinned (microcline)	Undetermined
420.6	34	9	12	1	12
431.3	19	5	10	1	3
435.3	28	5	13	0	10
436.8	19	3	9	0	7
439.5	33	7	15	1	10
441.0	14	4	8	0	2
442.0	19	5	7	0	7
443.5	7	3	2	0	2
445.0	23	6	9	1	7
445.3	14	5	5	2	2

nately, many lithologies represented by rock fragments are identifiable in thin section.

Sedimentary rock fragments are dominated by chert, which occurs as sand grains throughout the formation and as chert pebbles in layers near the top of the unit and in the base of the overlying Claggett Shale (fig. 8*A*). Several varieties of chert are common: one is clear, cryptocrystalline quartz free of any inclusions; another is deeply colored by opaque, carbonaceous material and contains numerous tiny euhedral crystals of pyrite. This latter variety may display spherical, elongate, or irregular internal structures, suggestive of microfossils. A third type of chert is brown or reddish-brown and contains numerous silt-sized grains of quartz or mica. This type is generally rich in isotropic material and might best be described as siliceous siltstone. In larger fragments or pebbles, some chert appears to be a siliceous breccia. Any of these chert fragments may be crosscut by chalcedony-filled fractures. Occasional tiny dolomite rhombohedra partially replace chert and may themselves be wholly or partly replaced by chalcedony. These features were probably produced long before erosion and transport. Many chert pebbles display a thin rind of black opaque material containing iron, magnesium, potassium, aluminum and silicon (D. D. Rice, personal commun., 1979). All the chert is composed of quartz of various crystal sizes, grading from truly cryptocrystalline quartz chert up to what would best be described as fine-grained polycrystalline quartz. This variation is often observed within a single fragment.

Other occasionally identified sedimentary rock fragments include siltstone, carbonaceous shale or claystone, siliceous shale, and fine-grained quartz sandstone (fig. 7*B*). Sand-sized grains of dolomite are

TABLE 7.—*Rock-fragment varieties counted in 10 selected core samples of Eagle Sandstone from the Bearpaw Mountains, Montana*

[Figures show number of grains]

Depth (m)	Sedimentary (including chert)	Metamorphic	Volcanic	Unidentified	Total grains counted
		30-1 Anderson core			
431.3	11	43	3	17	74
435.3	19	31	4	23	77
441.0	31	37	8	44	120
445.3	16	26	5	23	70
		29-3X Olson core			
521.5	30	18	0	25	73
527.6	30	20	2	24	76
531.9	14	16	1	16	47
534.0	54	17	0	21	92
535.8	27	25	1	30	83
538.3	29	30	12	19	90

also present and will be considered separately. Metamorphic rock fragments are the most abundant identifiable lithic component other than chert. These grains show considerable variation, which is apparent in all samples from all locations. Most are composed of quartz, white mica, and chlorite, with smaller amounts of biotite. The fragments may display well-developed schistosity. It is commonly possible to distinguish among metamorphic grains on the basis of the relative abundance of these components, as some are predominantly quartz while others contain mostly argillaceous material. Many quartz-rich fragments have textures that are probably relict sedimentary features, such as randomly oriented silt- or fine-sand-sized quartz crystals separated by a chloritic or micaceous matrix (fig. 7*C*). Argillites usually show a strong preferred optical orientation. Most metamorphic fragments can be classified as quartz-muscovite-chlorite schist, quartzite, or argillite, which includes slate, phyllite, and mica schist. In most identifiable fragments, mineral constituents suggest that the metamorphic sources were of a rather low grade, such as greenschist or low amphibolite facies, and that they represent a dominantly metasedimentary assemblage.

A few rock fragments in each sample are clearly of volcanic origin. The most easily recognized volcanic fragments consist of a dark, nearly isotropic groundmass, which may or may not be potassium-rich, containing one or more euhedral or fragmented euhedral phenocrysts of quartz (fig. 7*D*), K-feldspar, or plagioclase.

Many lithic fragments are not identifiable in thin section. Identification is particularly difficult for many dark, inclusion-rich, fine-textured grains, which are easily confused with sedimentary chert, and for highly altered lithic grains. Every sample also contains potassium-rich rock fragments that are nearly isotropic under crossed polars and that may contain crystals of potassium feldspar or plagioclase. These grains are commonly altered to potassium-rich clay and may contain quartz. In my opinion this sort of assemblage and alteration is probably volcaniclastic, like the anhedral, fine- grained fragments common in the Two Medicine Formation (Mudge, 1972, p. 74; Mudge and Sheppard, 1968). However, no definitive evidence was obtained, and the fragments are therefore labeled "unidentified" in this report.

DOLOMITE GRAINS

Numerous grains of dolomite constitute the only volumetrically significant nonsilicate component of the framework assemblage and may account for 5 or 10 percent of the rock. They are of approximately the same size as associated quartz grains and occur in point-to-point or line-to-line contact with adjacent framework silicates or as floating grains. Although some dolomite fragments may be polycrystalline, the majority are monocrystalline and display rounded rhombic morphology or subangular grain boundaries. Many of these exhibit twin lamellae and contain numerous black, nonmetallic, opaque inclusions. A small percentage of the dolomites contain readily identifiable polycrystalline or monocrystalline quartz (fig. 7*E*) or quartz chert. These silicate inclusions may be present in either monocrystalline or polycrystalline grains, which are otherwise indistinguishable from other dolomite fragments. A few grains are composed of approximately equal proportions of dolomite and quartz or quartz chert, with the rhombic dolomite crystals crosscutting older silicate textures. Yet even these grains display a rounded and abraded appearance, and in no case do the dolomite rhombohedra crosscut grain boundaries. These grains may bear a genetic relationship to previously described chert fragments which contain small automorphic dolomite rhombs as a minor replacement. No other types of silicate are observed within the dolomite grains. Wherever dolomite is present in a sample, the grains occur throughout the rock in approximately the same proportion, regardless of its postdepositional history. For example, in samples where calcite cement has been partially removed through dissolution, dolomite grains are equally abundant in the calcite-cemented and porous portions of the rock.

No evidence was observed to support an interpretation of intrastratal origin for the dolomite. Instead, the distribution, intergranular relationships, and morphology of these grains strongly suggest that they were deposited simultaneously with the remainder of the Eagle Sandstone framework assemblage. Internal textures and intragranular silicate relicts also suggest a detrital origin for the dolomite grains. This view is supported further by the presence of obviously detrital cobbles, pebbles, and sand grains of carbonate in the Two Medicine Formation (Mudge and Sheppard, 1968, p. 142; Mudge, 1972; Schultz and others, 1980). The Two Medicine is a continental equivalent of the Eagle Sandstone and, therefore, was presumably derived from the same sources.

This interpretation is at some variance with the views expressed by Sabins (1962) in his study of dolomite in Cretaceous sandstones of the Western Interior, including the Eagle Sandstone. He concluded that most monocrystalline dolomite grains that contain carbonaceous inclusions and display grain-to-grain contacts and abrasional features, are primary dolomite formed at the sediment-water interface not long prior to deposition of the remainder of the sediment.

COMMON VARIETAL CONSTITUENTS

Glauconite (used in the generic sense) is present in all but a few samples and may constitute a measurable percentage of the sand-size fraction. The glauconite occurs in the typical round or oblong microcrystalline grains of deep green color and relatively high birefringence. Internal structures are not usually seen, although occasional desiccation cracks are observed. Opaque inclusions are ubiquitous. No evidence of oxidation of iron in glauconite was noticed. Compaction has affected these grains to various degrees. Some examples display no evidence of glauconite deformation, while others are highly compacted. Original pelletoid morphology is generally best preserved in those samples where an early cement (calcite) has inhibited compaction. Glauconite is most abundant in sandstone containing measurable amounts of biotite. The pellets are entirely absent in nonmarine mudstones.

Biotite may account for as much as several percent of an entire sample and may be concentrated with other heavy grains in placer-like laminae. The mineral is commonly a deep brown color, although reddish brown or green biotite is also sometimes seen. The grains are generally very fresh but may locally be extensively expanded owing to clay mineral alteration. Biotite may also display a distinctive iron carbonate alteration, which is described in a later section. Compaction-produced biotite deformation is common.

Discrete muscovite fragments are much less common than biotite and rarely constitute as much as one percent of a sample. Muscovite is, however, a very important constituent of metamorphic lithic fragments and is far more abundant than biotite in these.

Detrital chlorite, displaying strong pleochroism, micaceous habit, anomalous interference colors (berlin blue) and, less commonly, sagenitic texture is observed in most thin sections. This chlorite may represent pseudomorphs of pre-existing ferromagnesian minerals such as biotite or hornblende.

HEAVY MINERALS

Except for biotite and chlorite, which are ubiquitous and plentiful, detrital heavy minerals generally constitute less than 0.2 percent of the framework grain assemblage. The nonopaque suite is dominated by apatite, zircon, garnet, and tourmaline, whereas magnetite and ilmenite are the only common opaque detrital grains. Grains of staurolite, rutile, orthopyroxene, and clinozoisite are rare.

Apatite usually occurs in rounded, prismatic, colorless grains and, less commonly, as angular fragments. Zircons are present in two populations: a perfectly euhedral, unabraded, clear form and a strongly rounded, pink or purple variety. The metamict and abraded condition of the latter variety suggests a probable Precambrian age. Garnets are generally rounded and colorless, with brown varieties less common. Angular fragments of garnet are also observed. Tourmalines are dominated by highly dichroic, well-rounded spherical or cylindrical grains of schorl. However, less pleochroic varieties are not unusual.

SOURCES OF THE EAGLE SANDSTONE

In the vicinity of the Bearpaw Mountains, the Eagle Sandstone was deposited along a north-northwest-trending shoreline, during one of the periodic uplifts that occurred in western Montana throughout the Cretaceous. Regional stratigraphic relations, sandstone distribution, and ammonite zone trends all suggest that the sediments had a westerly source. The materials were delivered to the shore through small deltas and transported for short distances by a southward-flowing longshore current (Rice, 1980).

The metamorphic assemblage, which comprises the most abundant identifiable lithic component within the Eagle Sandstone, probably accounts for a large portion of the quartz grains as well. Observable fragments indicate the argillaceous and siliceous metasediments originally consisted of mudstones, shales, siltstones and fine-grained

sandstones. Framework grains of quartz and feldspar in these sediments were largely unaffected by metamorphism, whereas clay components were altered to white mica and chlorite and, less commonly, to biotite. These properties suggest derivation from large exposures of the Belt Supergroup in orogenic highlands to the west. At present, the Belt Supergroup in northwestern Montana contains from 2,135 to 15,250 m (Mudge, 1970, p. 378) of argillaceous, quartzitic, and carbonate rocks displaying low-grade regional metamorphism (Ross, 1963). These lithologies agree well with those observed in the metasedimentary components of the Eagle Sandstone. Even today, very few exposures of pre-Belt crystalline rocks are present in western Montana.

Fragments of chert, detrital dolomite, and very fine grained quartzarenite are abundant in the Eagle Sandstone, and siliceous shale, carbonaceous shale, and mudstone are common, demonstrating that sedimentary rocks were an important part of the source terrane. Although some of these materials were almost certainly derived from the Belt Supergroup, the abundant chert and dolomite fragments probably resulted from the rapid erosion of Paleozoic sediments. The whole Paleozoic section presently exposed in the Sun River Canyon area is approximately 1,220 m thick and is dominantly composed of carbonate rocks, many of which are dolomitic and cherty (Mudge, 1972). In that area, chert- bearing dolomites in the Mississippian Castle Reef Dolomite are from 75 to more than 305 m thick (Mudge, 1972). Other sedimentary materials in the Eagle could have been eroded from Mesozoic rocks or could represent intraformational erosion. However, no definitive evidence was documented for these sources.

Volcaniclastic material is ubiquitous in the Eagle Sandstone. Distinctive bipyramidal quartz grains and some lithic fragments are clearly volcanogenic. Similarly, the abundant subhedral and fragmented grains of sanidine are indicative of a shallow intrusive or extrusive origin. Other components, such as andesine, biotite, orthoclase, and the common unidentified isotropic rock fragments, may have had similar origins.

The exact location and nature of the contributing volcanic sources for the Eagle Sandstone are not known. Volcanism occurred sporadically during the later Mesozoic in western Montana and adjacent areas, yielding sediments to the Kootenai Formation (Aptian) and to the Vaughn Member of the Blackleaf Formation (upper Albian) prior to deposition of the Eagle Sandstone. Sources for these volcanogenic materials are believed to have lain to the west of the present mountain front in areas now buried by thrust plates in the vicinity of the Lewis and Clark Range (Mudge and Sheppard, 1968). Similar vol-

canic rocks and volcaniclastic sediments may have been exposed to erosion during accumulation of the Eagle Sandstone. Late Cretaceous volcanism began no later than Santonian time in western Montana, when the Slim Sam Formation, a sequence of volcano-sedimentary rocks, was deposited conformably upon the marine Colorado Shale (Klepper and others, 1957, p. 28; Smedes, 1966, p. 13). The transitional Slim Sam Formation grades upward into the Elkhorn Mountains Volcanics, an accumulation of calcalkaline extrusive and shallow intrusive rocks, which once covered as much as 25,900 km^2 of western Montana (Smedes, 1966, p. 21). The lower part of the Elkhorn Mountains Volcanics may be as old as the Telegraph Creek Formation (Klepper and others, 1957, p. 32) and is almost certainly contemporaneous, in part, with the Eagle Sandstone (Smedes, 1966, p. 27). The lower portion of the Elkhorn Mountains Volcanics is dominantly andesitic or rhyodacitic in composition and contains phenocrysts of quartz, orthoclase, and intermediate plagioclase (Smedes, 1966). These phenocrysts are petrographically similar to certain components of the Eagle Sandstone. The Elkhorn Mountains volcanic center definitely contributed clastics to the Eagle Sandstone in the Livingston, Mont., area (Roberts, 1972, p. 31). It is tempting to invoke the Elkhorn Mountains as a source for volcaniclastic material in the Eagle Sandstone of the Bearpaw Mountains area as well. However, this volcanic field may have lain too far southward to have actively contributed to the westerly sources of the Eagle Sandstone there. While derivation from the Elkhorn Mountains Volcanics cannot be positively discounted, sources in volcanic rocks to the west, now buried by thrust plates, and in older volcanic complexes and volcaniclastic sediments are also likely candidates.

Plutonic rocks may have served as sources for the Eagle Sandstone, but their presence is not unambiguously demonstrated by the mineralogical evidence. Intermediate plagioclase and orthoclase, both common to the Eagle, are probably igneous in origin. These feldspars could have been derived from either a plutonic or a volcanic terrane. The striking scarcity of microcline might suggest that plutonic materials were unavailable. However, many of the great Cretaceous batholiths of the northwest had been in place for tens of millions of years by the beginning of Eagle Sandstone deposition and could have been exposed to erosion in Campanian time. The Idaho batholith, dated at between 92 and 135 m.y. by the lead-alpha method (Larsen and others, 1958), and the Nelson batholith of British Columbia, dated by the K-Ar method at 96 m.y. (Baadsgaard and others, 1961), are both located in likely source areas for Eagle Sandstone sediments. Descriptions by Cairnes (1934) and Little (1960) suggest that most coarse-grained potassium feldspars in the Nelson batholith are

orthoclase rather than microcline. Larsen and others (1958) report large volumes of rock in the Idaho batholith with orthoclase phenocrysts, although some plutons apparently do contain coarsely crystalline microcline.

DIAGENESIS

Postdepositional processes have operated extensively within the Eagle Sandstone in the Bearpaw Mountains area. Petrologic investigations indicate that the high porosity and permeability of the rock, which make it a good conventional gas reservoir, were not entirely developed during deposition, but rather, that intrastratal effects operating throughout the burial history of the unit have played a dominant role. These effects have been reasonably simple and consistent throughout the study area. This consistency reflects the uniform biological processes, relatively shallow burial depths, and regionally similar orogenic activity in the Bearpaw Mountains area. This section describes observed postdepositional features within sandstone units of the Eagle Sandstone and discusses the processes that were responsible for them. Table 8 summarizes the inferred burial history of the Eagle Sandstone and the evidence upon which it is based.

CALCITE

Calcite cement tightly seals only a relatively small volume of the Eagle Sandstone, typically occupying layers a few tens of centimeters thick. These layers are readily identifiable in electric logs (fig. 2) and are apparent as resistant ledges in outcrop. Cemented layers are present in almost every section of the Eagle Sandstone, but all sections contain a larger volume of rock that is incompletely cemented. Where layers are completely cemented with calcite, this cement composes 30 percent or more of the rock volume.

The results of stable-carbon-isotope analyses of seven selected samples of calcite cement and one sample of a calcareous concretion are presented in table 9. The samples were collected from three cores of the Eagle Sandstone: 30–1 Anderson, 29–30X Olson, and No. 1 Federal (table 1). All eight samples yielded significantly and consistently negative $\delta^{13}C$ and $\delta^{18}0$ values relative to the PDB Chicago standard, ranging from -6.52 to -7.56 permil for carbon and -13.83 to -15.65 permil for oxygen. These values suggest equilibration with meteoric waters. However, the mechanism by which the isotopically light carbon and oxygen were incorporated in the calcite is not known.

TABLE 8.—*Summary of Eagle Sandstone burial history*

No.	Event	Evidence
1	Deposition----------	
2	Pyrite formation----------	(1) Pyrite is included, along with organic matter, in early-formed calcite. (2) Inference based on chemical requirement of sulfate reduction for bacterially generated methane.
3*A*	Methane generation----------	Inference based on modern occurrences of biogenic methane generation (Claypool and Kaplan, 1974) and on carbon isotope composition of gas.
3*B*	Precipitation of early calcite cement.	(1) Calcite contains abundant organic and pyritic inclusions (fig. 8*A*). (2) No preexisting authigenic phases are crosscut by this carbonate. (3) Included detrital grains display no evidence of compactional deformation. (4) Cement occupies 40 percent or more of rock volume. (5) Calcite displays fabric and optical qualities of concretions observed in the Eagle Sandstone.
4	Compaction and minor quartz cementation.	(1) Quartz overgrowths are often associated with somewhat compacted soft grains such as glauconite or biotite. (2) Sparry calcite fills fractures in framework grains and in inclusion-rich calcite cement (event 3*B*). (3) Quartz overgrowths are marginally embayed by sparry calcite cement (event 5*A*).
5*A*	Extensive precipitation of and replacement by sparry calcite.	(1) Sparry calcite embays quartz overgrowths. (2) Sparry calcite fills fractures in framework grains and in inclusion-rich calcite (event 3*B*). (3) Carbonate surrounds somewhat compacted grains of biotite and glauconite. (4) Extent of calcitization indicated by dissolution textures (event 6).

5*B*	Siderite formation associated with biotite.	(1) Siderite is associated with calcite or with evidence of preexisting calcite. (2) Siderite appears to crosscut calcite cement textures. (3) Siderite is generally associated with disrupted biotite (fig. 10*A*).
6	Calcite dissolution----------	(1) Ubiquitous calcite relicts in intragranular and intergranular pores (fig. 8*F*). (2) Dissolution fabric at margins of calcite and voids in optically continuous calcite (fig. 8*C*). (3) Application of textural criteria of Schmidt and others (1978) to porous portions of the Eagle Sandstone.
7	Precipitation of abundant siderite near top of 29-3X Olson core.	(1) Rhombohedra of siderite are perfectly fresh and euhedral (fig. 10*E*). (2) Siderite occupies dissolution features in quartz overgrowths (fig. 10*E*). (3) Siderite occupies voids interpreted as dissolution features in calcite. (4) Siderite rhombs crosscut fabric of sparry calcite and quartz overgrowths.
8*A*	Authigenic clay formation---	(1) Kaolinite occupies voids in optically continuous calcite cement.(2) Kaolinite overlies authigenic quartz and authigenic siderite (fig. 10*E*).
8*B*	Major migration of economically significant quantities of biogenic methane from associated sediments.	Inferred on basis of presence of authigenic tourmaline observed by Gautier (1979), which indicates migration subsequent to tourmaline precipitation during Bearpaw Mountains uplift and volcanism.

TABLE 9.—*Carbon and oxygen isotope data for selected samples of Eagle Sandstone carbonates*

[Expressed in parts per thousand $_{\delta}$ relative to the PDB Chicago standard. N indicates no determination]

Core	Depth (m)	$\delta^{13}C$	$\delta^{18}O$
Determinations on calcite			
29-3X Olson	532.8	-7.54	N
Do-------	532.8	-7.56	N
30-1 Anderson	439.8	-7.33	N
Do-------	443.2	-7.40	N
Do.[1]-----	429.8	-6.58	-15.65
No. 1 Federal	424.7	-7.23	-15.55
Do-------	425.0	-6.52	-13.83
Do-------	426.6	-7.34	-15.31
Determinations on siderite			
29-3X Olson--	518.2	-0.99	N
Do-------	520.0	-1.21	N

[1]Calcite concretion.

Calcite has two basic modes of occurrence. The first is a fine-grained, inclusion-rich variety. The second is a coarsely crystalline, clear, sparry variety (fig. 8*A*).

The first type of calcite appears as a finely crystalline mosaic, in patches, filling intergranular spaces. These patches are generally cloudy, owing to abundant inclusions of organic material. Blebs and grains of anhedral to euhedral pyrite may be sparsely disseminated within it. Framework grains within the rocks cemented by inclusion-rich calcite generally display little evidence of compaction. Grain contacts are most often tangential, but many framework grains appear to "float" in calcite. The fine-grained carbonate may exist in areas larger than the combined diameters of several framework grains. In these more extensive areas, the fine-grained crystals are organized such that the entire patch displays radial extinction, similar to that observed in the calcite concretions that are occasionally seen in the Eagle Sandstone. Where carbonate development has been most extensive, clastic grains are generally excluded and glauconite, if present, may be seriously disrupted or replaced by the calcite. Excepting pyrite, no diagenetic effects were observed to precede this mineral.

Most calcite occurs as a clear, coarse, sparry mosaic of anhedral crystals, typically 0.1 mm in diameter or larger, which may poikilo-

topically enclose silicate framework grains over large areas of the thin section. This carbonate is only rarely twinned and is generally free of inclusions. In addition to occupying intergranular spaces, it may fill fractures if they are present. A few of these rare calcite-filled fractures cut across areas of fine-grained, organic-rich calcite, thus demonstrating the paragenetic relationship between the two calcite varieties. Easily deformed grains, such as glauconite, may show evidence of compaction in rocks cemented with sparry calcite. Micaceous grains or argillaceous lithic fragments are commonly undeformed. Labile constituents, such as feldspars and volcanic rock fragments, are perfectly preserved by the carbonate cement, displaying no clay alteration or dissolution effects. Calcite does, however, partially replace some clastic silicates, particularly plagioclase. It tends to follow cleavage planes and fractures within the grain. This replacement results in wedgelike, rhomboid, or irregular areas of calcite within the silicate fragment (fig. 8*B*). The carbonate completely fills intergranular pores. The calcite commonly embays the margins of quartz, feldspars, and other silicates, producing "caries-type" boundaries. Where calcite cement is extensive, other cements or replacements are rare, although minor preexisting quartz overgrowths may be observed in areas of sparry cement.

Near the upper or lower boundaries of the calcite-cemented layers, close to the more common highly porous portions of the sandstone, voids are apparent within the intergranular cement (fig. 8*C*). The voids farthest inside the cemented zone appear in the centers of intergranular spaces and exhibit the ragged boundaries characteristic of dissolution features within a formerly complete crystal mosaic rather than the clear, sharp boundaries that would result from incomplete cementation. In the more coarsely grained cement these pores occur within optically continuous crystals. It is concluded that these voids result from partial dissolution. Even closer to the porous portions of the sandstone calcite dissolution effects are more intensive. Fully open intergranular pores appear, bounded by slightly embayed framework materials. These pores contain small remnants of the once-continuous cement, now reduced to a few patches of completely isolated carbonate, which may still display optical continuity. Intragranular pores partly occupied by remnant calcite are also seen. These are most often present in plagioclase feldspars (fig. 8*D*). The intragranular pores are morphologically similar to the framework replacement features of calcite observed in completely cemented rocks, with voids often following cleavages or displaying wedgelike or rhombic outlines. These intragranular pores may be so extensive as to leave only skeletal remnants of the original framework silicate (fig. 8*E*). These remnants are often surrounded by tiny relicts of the

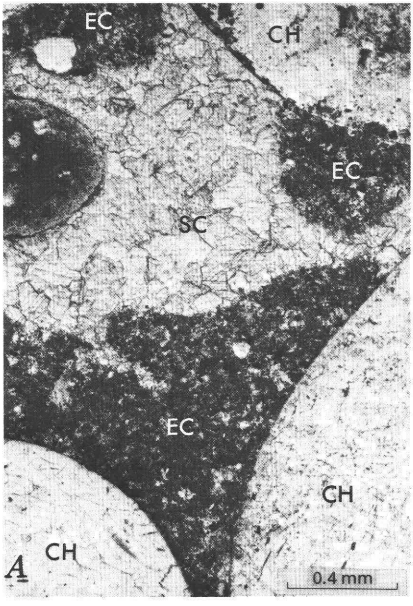
EC
CH
EC
SC
EC
CH
CH
A
0.4 mm

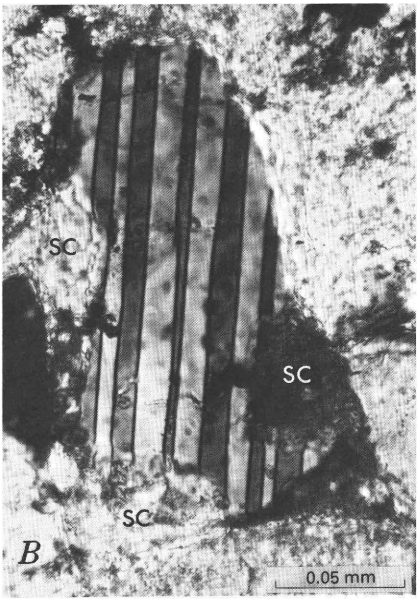
SC
SC
SC
B
0.05 mm

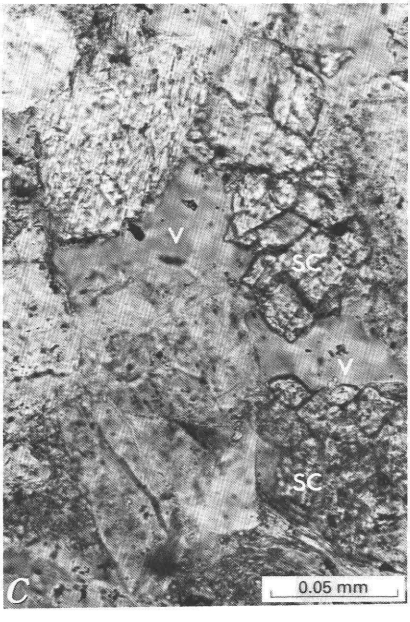
V
SC
V
SC
C
0.05 mm

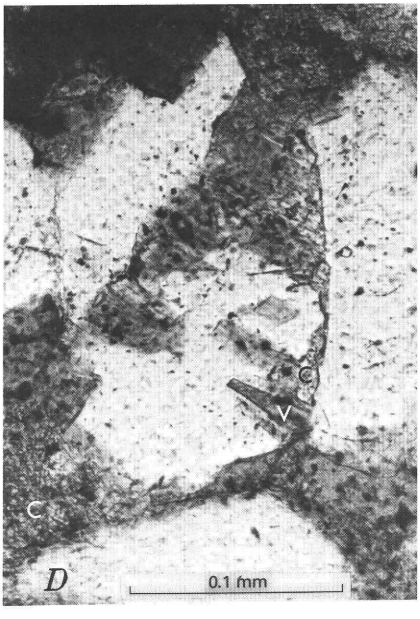
C
V
C
D
0.1 mm

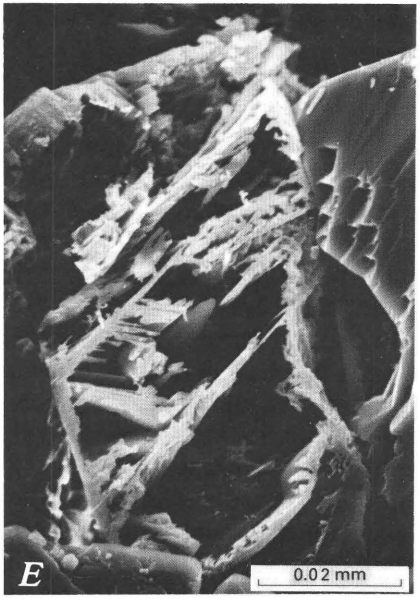

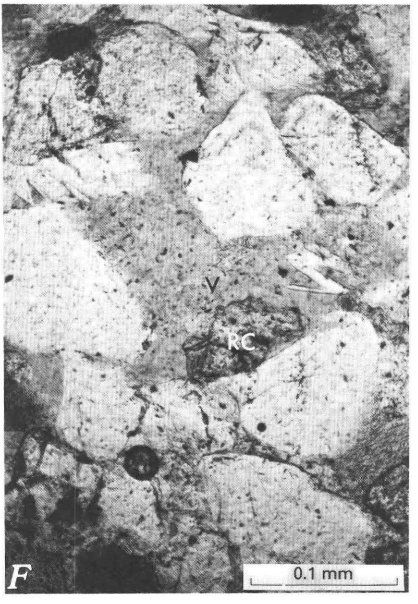

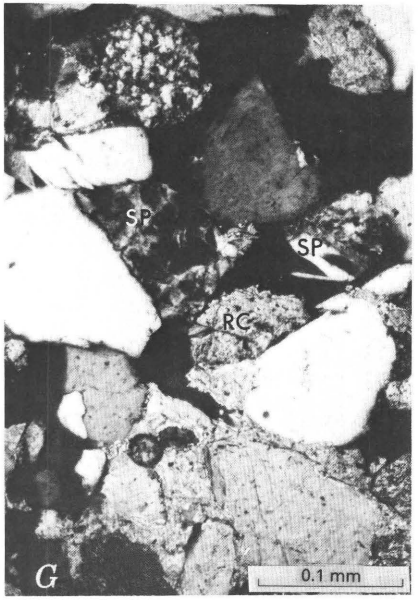

FIGURE 8.—Dissolution and calcite replacement features of the Eagle Sandstone. *A*, Chert-pebble (CH) conglomerate, from near top of Eagle Sandstone, cemented by two types of calcite: inclusion-rich, fine-grained early carbonate (EC) and later sparry calcite cement (SC). (Crossed polars.) *B*, Partial replacement of albite-twinned plagioclase by sparry calcite (SC). (Crossed polars.) *C, Dissolution voids (V) in optically continous sparry calcite cement (SC) (Plane light.) D*, Angular dissolution voids (V) in plagioclase, associated with relict calcite (C) replacement and cement. (Plane light.) *E*, Skeletal remnant of plagioclase grain. (SEM photomicrograph.) *F*, Oversize pore (V) containing relict calcite (RC). (Plane light.) *G*, Same view as 8*F*, showing skeletal remnants of plagioclase (SP). (Crossed polars.)

replacement calcite, which has been almost completely removed by dissolution (fig. 8*F*, *G*).

The highly porous, permeable rocks contain a small (<<1 percent) but ubiquitous component of relict calcite, which occurs in either intergranular or intragranular spaces. The intergranular pores are of disparate sizes, including typical triangular-type intergranular voids connected by elongate passages. The grain boundaries along these pores may display the same development of caries texture seen in calcite-cemented rocks. Intragranular voids are extensive in the highly porous rocks. Nearly complete plagioclase grains grade into distinctly delicate skeletal remnants of plagioclase (fig. 8*E*), which grade into large voids containing only a few bits of silicate material (fig. 8*F*, *G*). Large pores, larger than the size of most sand grains, are also present. It is likely that these oversize pores were once partly occupied by a framework silicate, probably plagioclase, or by a large patch of fine-grained calcite. A continuous gradient of dissolution may thus be observed, ranging from completely cemented rocks into the highly porous and permeable sandstones.

This petrographic evidence indicates that the fine-grained calcite formed prior to the sparry cement. Its finely crystalline texture and abundant organic inclusions indicate that it precipitated early in the burial history of the rock, probably immediately following deposition. Sparry calcite developed after some compaction had occurred and after the development of minor quartz overgrowths, which may have tacked together the quartzitic framework grains.

The gradational transition from calcite-cemented to highly porous sandstone, the observable dissolution features in the calcite cement, and the presence of relict calcite within the highly porous rocks are unequivocal evidence that calcite once occupied a far larger volume of the Eagle Sandstone than at present. The minimum volume of sandstone once cemented by carbonate may be estimated from the present distribution of relict calcite (compare fig. 6 and fig. 9). The maximum volume formerly occupied is less easy to determine, however. In a highly influential paper, Schmidt and others (1977, p. 275) illustrated petrographic criteria applicable to the determination of the presence of secondary porosity. These include (1) partial dissolution of calcite cement, (2) molds of former framework grains, (3) inhomogeneous packing, (4) oversized pores and floating grains, (5) elongate intergranular pores, (6) corroded grain margins, (7) honeycombed grains, and (8) fractured grains (Schmidt and others, 1977). Every one of these criteria can be observed in most of the highly porous and permeable rocks of the Eagle Sandstone. The application of these criteria to the samples from the 30–1 Anderson core, for example, would indicate that a sequence of calcite cementation and replace-

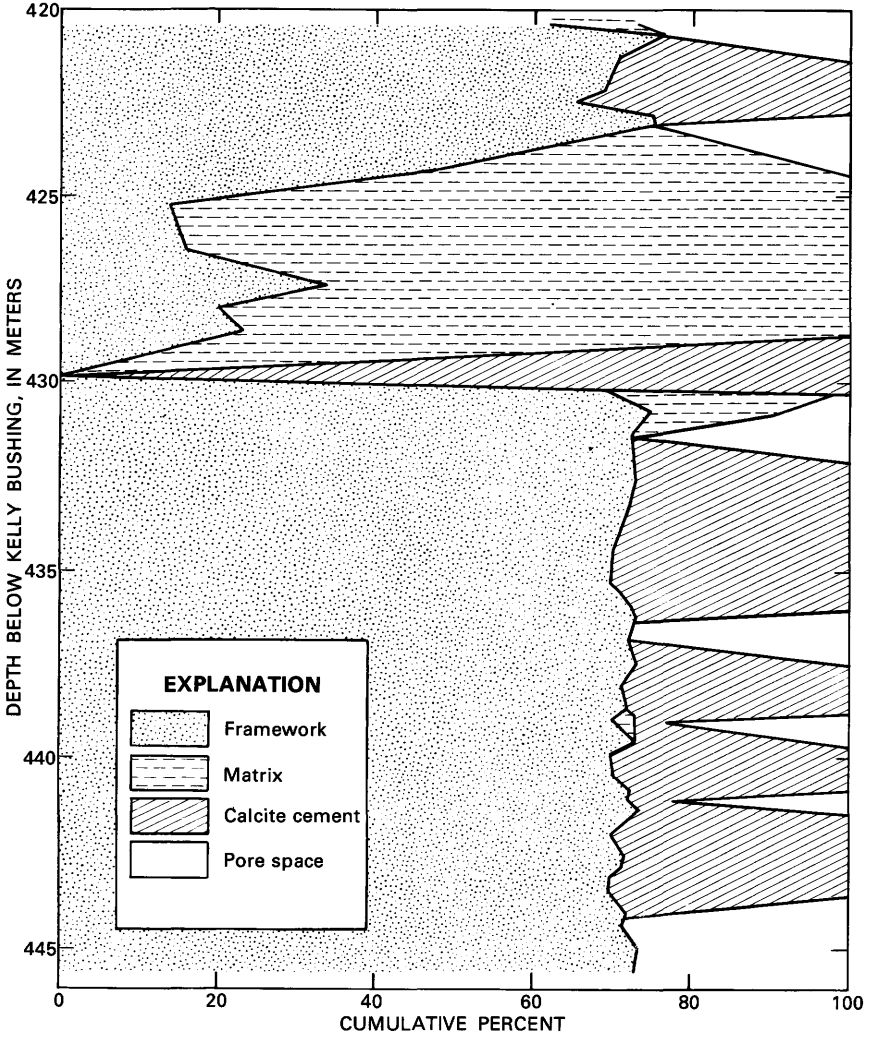

FIGURE 9.—Estimated framework, matrix, cement, and pore space distribution based upon minimum volume of calcite present prior to dissolution.

ment followed by calcite dissolution has produced most of the observable pores (fig. 9).

Two interpretations seem to explain the present calcite distribution and accompanying textural qualities. The first is that calcite at one time simultaneously occupied most pore spaces in the Eagle Sandstone This theory suggests that the present-day conventional reservoirs were once completely tight nonreservoirs. If such were the

case, the calcite must have been subsequently removed by dissolution processes which operated nearly everywhere, leaving only isolated remnants of the formerly extensive cement. This inference demands that the gas now occupying these reservoirs has migrated into the rocks since the dissolution of the carbonate, thus placing rather dramatic constraints upon reservoir quality and the timing of gas migration. This interpretation effectively explains the present textural properties of the formation as well as the observed distribution of calcite relicts and dissolution features throughout the rock. It requires, however, an explanation of where all the original calcite came from and where it has gone. It fails to account for the mechanism by which water moved through what would have been an impermeable rock and effectively dissolved most of the calcite cement while leaving isolated discrete ledges of carbonate. Furthermore, it does not account for the seemingly inexplicable absence of completely cemented Eagle Sandstone which, it would seem, should be preserved somewhere in the Bearpaw Mountains area. Finally, it does not explain where the methane was during the time the reservoir was tightly sealed. Since the gas was certainly generated very early in the burial history, it must have occupied some reservoir during the time of calcitization. No such storage place exists, however, to my knowledge. This latter argument could be circumvented if the methane had remained in solution from the time of generation until after the dissolution of calcite.

An alternative interpretation, also consistent with the petrographic evidence, is that calcite has at one time or another occupied virtually every pore in the reservoir but that at no time did it simultaneously occupy the entire rock. In this case, the distribution of calcite during much of the burial history of the Eagle Sandstone might have been very similar to that observed today.

Layers, ledges, and patches of authigenic carbonate in sandstones are common in the geologic record. One explanation of their occurrence is based upon the nonlinear solubility of ionic compounds as a function of various geochemical parameters, such as the concentration of dissolved neutral electrolyte (Runnells, 1969), the partial pressure of carbon dioxide (Bogli, 1964), common-ion effects (Runnells, 1969), the concentration of dissolved organic compounds, and pH. Precipitation of calcite can occur from essentially undersaturated waters wherever they become locally supersaturated with respect to calcite. This local supersaturation may develop near chemical or physical interfaces or along chemical gradients whenever any of the critical parameters are affected. Because chemical interfaces or gradients are almost never static in nature, their movement may produce a sequence of precipitation and dissolution throughout their

path. Effects of this movement may be preserved as petrographic evidence. Specific mechanisms of this sort that could feasibly have operated during the burial history of the Eagle Sandstone include movement of the gas-water contact and the mixing of natural waters, as described by Runnells (1969), along the shoreline early in the burial history or within the formation during later burial and uplift.

I believe this interpretation successfully explains the ubiquitous presence of cemented layers throughout the Eagle Sandstone and accounts for the absence of any large volumes of tightly cemented rocks in the formation. This mechanism also explains the origin of calcite dissolution features and the apparent former presence of calcite throughout large portions of the reservoir. This mechanism requires only small amounts of carbonate to be present at any one time; thus it avoids the invocation of seemingly catastrophic events of cementation and replacement followed by equally catastrophic dissolution, and it does not exclude the occupation of the reservoir by methane. A proposed mechanism of continual precipitation and dissolution would be expected to effectively homogenize divergent carbon isotope contents, thus producing isotopic compositions consistent with those observed within the calcites of the Eagle Sandstone.

As in most cases where the former presence of extensive replacement or cementing minerals can be documented, petrographic relationships yield little information about the absolute timing of such events. Thus, the simultaneity of calcitization throughout the Eagle Sandstone is not definitively demonstrated. Rather, calcite can only be placed within a relative paragenetic framework, mostly postdating compaction and quartz cementation (except for the earliest calcite) and preceding calcite dissolution and clay mineral development (table 8). A final determination of which model best explains the observed petrographic properties of the Eagle Sandstone is not possible at present, although I favor the latter, nonsimultaneous interpretation. A possible means of testing the various hypotheses is suggested by the computer models of carbonate dissolution and precipitation during natural water mixing developed by L. N. Plummer (1975).

IRON CARBONATE

Iron-rich carbonate phases identified by X-ray diffraction analysis as siderite or, less commonly, as ankerite are present in most samples in amounts ranging from a trace to several percent of the rock volume. These ferrous minerals typically occur as accumulations of tiny subhedral, golden crystals in patches a few tenths of a millimeter in diameter. The carbonate is often associated with biotite and, less commonly, with detrital chlorite in various stages of preservation.

This relationship covers a continuous spectrum ranging from fresh, reddish-brown biotite in which a few rhombohedra of iron carbonate have formed between cleavage plates to massive accumulations of crystals containing a few small fragments of widely dispersed biotite (fig. 10*A*). Some areas of iron carbonate contain no detectable relict biotite, and many biotite grains display no carbonate alteration. These effects may be observed in either calcite-cemented or highly porous rocks. The paragenetic placement of the formation of this iron carbonate is tenuous, but the crystals appear to cut across preexisting calcite cement textures, suggesting that the iron carbonate formed later than some of the calcite.

The upper portion of the 29–3X Olson core contains morphologically distinct iron-rich carbonate in far greater abundance than is typical for the Eagle Sandstone as a whole. In addition to forming small localized patches, fine-grained carbonate has developed extensively in some areas, where it may fill most intergranular pores, largely replace framework grains, and locally develop into widespread accumulations containing no silicate material at all. X-ray diffraction analysis of this fine-grained iron carbonate indicates it is composed entirely of siderite ($d_{10\bar{1}4}$=2.81 A). Qualitative compositional information, obtained with an X-ray energy-dispersive spectrometer attached to an SEM, indicates that the variance in d-spacing, compared with $d_{10\bar{1}4}$=2.79 A for pure $FeCO_3$, results from the isomorphous entry of $CaCO_3$ into the siderite. This type of substitution is known to produce a slight expansion of the crystal lattice (Zaritskiy, 1964). Stable carbon isotope analyses from two samples of this mineral indicate it possesses a carbon isotope ratio of about zero, relative to the PDB standard (table 9).

More coarsely grained siderite also occurs in the 29–3X Olson core: as clear brown rims formed in crystallographic continuity with dolomite fragments (fig. 10*B*) and as discrete, perfectly euhedral rhombohedra 0.004 to 0.01 mm in diameter. The rhombohedra are disseminated throughout some samples and tend to be concentrated along intergranular pores, some of which are interpreted as having resulted from calcite cement dissolution. The crystals are uncommon in areas of extensive calcite and do not occur within intragranular pores in framework silicates. However, the rhombs may automorphically cut across most mineral phases within the sandstone, including calcite. The scanning electron microscope reveals that the rhombic crystals of siderite display absolutely no evidence of dissolution etching and appear to have formed later than the embayments in the quartz, which they may partly occupy (fig. 10*C*). Kaolin crystals in well-developed booklets commonly have formed upon the euhedral siderite crystals (fig. 10*D*). Thus, textural relationships indicate that the

coarsely crystalline siderite definitely developed prior to authigenic kaolin and may postdate calcite precipitation and dissolution.

The chemical requirements for the precipitation of siderite from solution and the equilibrium conditions controlling the chemical relationships among iron minerals in the presence of dissolved carbon, sulfur, and iron species have been discussed by Garrels and Christ (1965, p. 201–225). According to their calculations, the formation of siderite under ideal conditions at moderate pH values requires a very low oxidation potential, which permits high ferrous iron activities, a high bicarbonate activity, and very low values for total dissolved sulfur. Under such conditions ferrous carbonates may be stable in the presence of ferrous sulfides such as pyrite. The relationship between calcite and siderite is simple under ideal conditions and is governed by the following relationship:

$$CaCO_{3_{cryst}} + Fe^{+2}_{aq} = FeCO_{3_{cryst}} + Ca^{+2}_{aq},$$

or

$$K_{eq} = [Ca^{+2}]/[Fe^{+2}],$$

where K_{eq} is the equilibrium constant. The value obtained for K_{eq} depends upon whose thermodynamic data are used in evaluating the relationship and may vary between 150 (Krauskopf, 1967, p. 83) and 794 (calculated from free energy of formation values given by Garrels and Christ, 1965). In any case, siderite may be formed from calcite whenever significant amounts of ferrous iron are present. For example, using the K_{eq} value given by Krauskopf, if the activity of dissolved calcium is equal to 10^{-1}, siderite should precipitate under ideal equilibrium conditions at dissolved ferrous iron concentrations of about 0.7 moles per liter. If thermodynamic values cited by Garrels and Christ are used, this value drops to about 0.1 moles per liter.

In most samples of the Eagle Sandstone, iron carbonates were found mainly in localized patches, associated with detrital biotite (fig. 10*A*). This pattern of occurrence is regarded as strong evidence that the biotite has yielded iron from its lattice to its surroundings, facilitating siderite formation. This process may be analogous to the movement of iron from ferromagnesian minerals under oxidizing conditions, as reported for Cenozoic sediments of the Sonoran Desert (Walker and others, 1967). While the diffusion gradient thus created will produce ferric oxides and hydroxides under aerated conditions like those observed by Walker and others, a similar chemical gradient under conditions of high bicarbonate activity and very low oxidation potential would produce an iron carbonate such as siderite. In the case of calcite-cemented Eagle Sandstone, it is likely that the development of an iron diffusion gradient away from a source of iron, such

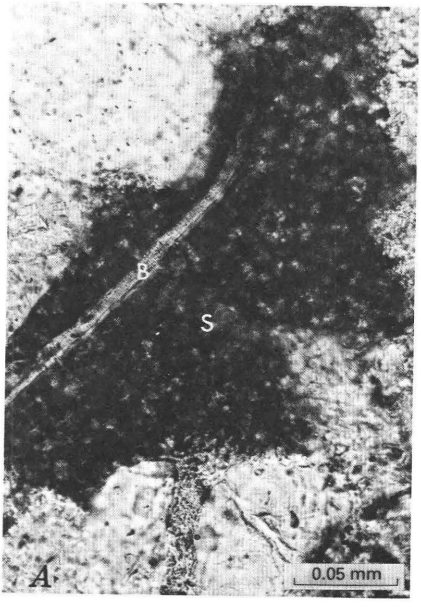

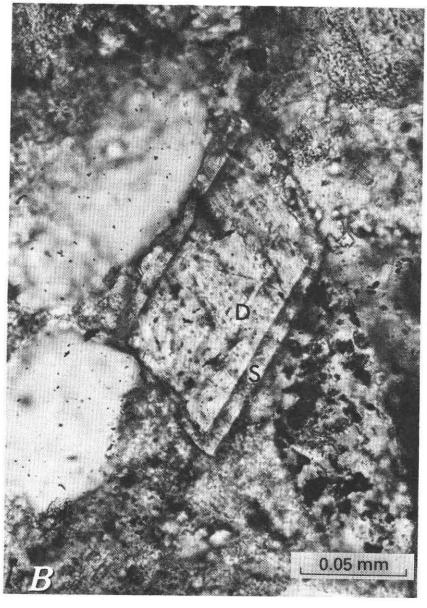

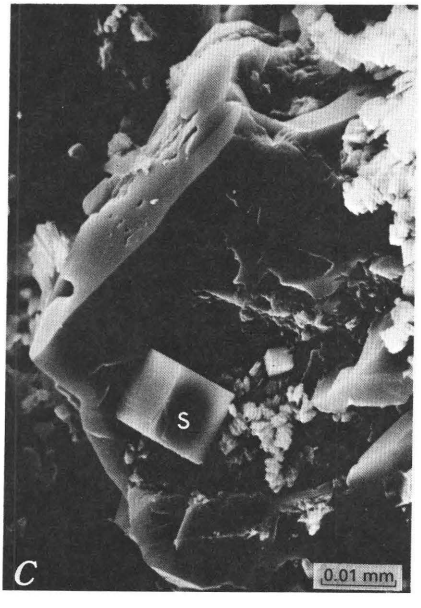

FIGURE 10.—Noncalcitic authigenic minerals in the Eagle Sandstone. *A*, Mass of siderite (S) associated with remnants of altering biotite (B). (Crossed polars.) *B*, Rim of authigenic siderite (S) in optical continuity with monocrystalline grain of detrital dolomite (D). (Plane light.) *C*, Euhedral rhombohedron of siderite and kaolin booklets in embayed quartz overgrowth. (SEM photomicrograph.) *D*, Authigenic kaolinite (K) precipitated on surface of authigenic siderite (S). (SEM photomicrograph.) *E*, Kaolinite booklets in an intergranular pore. (Plane light.)

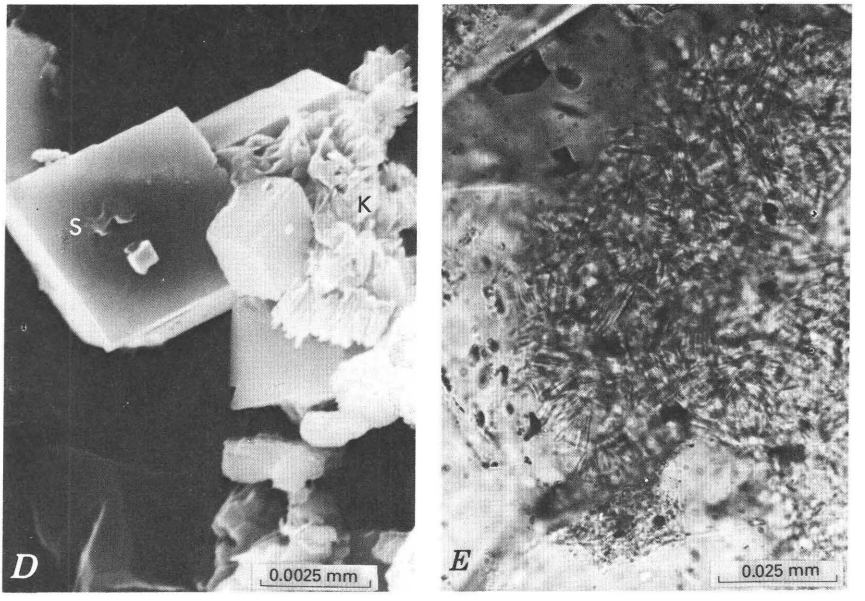

as biotite, would raise the ferrous iron activity in the vicinity of the biotite to levels sufficient to locally replace the calcite cement with siderite. It is reasonable, therefore, that the formation of local siderite patches within the carbonate- cemented Eagle Sandstone occurred once iron became locally mobilized by the breakdown of biotite.

The extensive occurrence of siderite observed in the upper portion of the 29-3X Olson Core, however, cannot be explained in this fashion. The production of such large quantities of iron carbonate apparently required the introduction of iron from an external source, as insufficient amounts are present within the detrital constituents of the Olson core. Carbon isotope data (table 9) suggest an episode of formation separate from and unrelated to calcitization. Speculation about this iron source would probably be fruitless except to point out that stratigraphically equivalent rocks, such as the Gammon Member of the Pierre Shale farther east and the Virgelle Sandstone near the Montana disturbed belt, are also iron-rich. The Gammon contains abundant ferruginous concretions, and the Virgelle Sandstone displays prominent placer-like concentrations of magnetite. In

addition, in the vicinity of the Bearpaw Mountains, the Eagle Sandstone may display ferruginous cements in outcrop. These ferruginous zones may have developed from the oxidation of siderite during weathering. Whether these occurrences are genetically related or only coincidental is not known.

INTRAGRANULAR POROSITY

Dissolution processes have produced significant amounts of intragranular porosity within framework grains of the reservoir sandstones. Point counts indicate that many samples contain intragranular pore space in volumes equal to or even in excess of intergranular pore volume. Most of this dissolution has affected plagioclase feldspars, although minor intragranular voids may be observed in quartz, potassium feldspar, or dolomite grains. Dissolution features range from wedgelike, rhombic, or irregular voids within otherwise pristine andesine fragments (fig. 8*D*) or small embayments in quartz grain margins, to voids the size of framework grains that contain only a few scattered remnants of the original silicate structure (figs. 8*E, G*). Occasional observations of authigenic kaolinite enclosing grain-size voids (moldic porosity), of oversize pores, and of inhomogeneous packing of framework grains demonstrate that framework silicates have been completely removed by dissolution processes.

The removal of framework grain material may be largely accomplished by the dissolution of calcite that had previously replaced silicate grains. The preferential replacement of plagioclase by calcite and the resultant proliferation of intragranular voids in these feldspars suggest an affinity of the carbonate for the calcium-bearing plagioclases. Schmidt and others (1977) expressed the view that most secondary intragranular pores are formed by dissolution of carbonates. However, the direct dissolution of detrital and authigenic silicates has been demonstrated by Walker, Waugh, and Crone (1978, p. 19–32) and by Heald and Larese (1973), among others. This process may produce significant amounts of pore space, particularly in sandstones containing a large proportion of labile constituents such as volcaniclastic material (Hayes, 1979; Hayes and others, 1976). Evidence for the development of porosity through the direct dissolution of silicate grains is also present in the Eagle Sandstone. For example, in argillaceous sandstones and mudstones, where a former episode of extensive calcitization cannot be demonstrated, skeletal remnants of plagioclase grains are occasionally observed. Such remnants reflect instances where intragranular pores developed through direct plagioclase dissolution.

Experimental work by Lagache and others (1961a, b) and Wollast (1967) resulted in a theory of feldspar dissolution kinetics, which is summarized by Helgeson (1971), who developed a rate law for the dissolution. In general, at low temperatures and pressures, plagioclase dissolution is controlled by the outward diffusion of the large cations (Na, Ca). Where the hydrogen ion concentration is moderate, the dissolution rate depends upon the amount of grain surface area exposed and the rate of movement of migrating dilute solutions. Under these conditions, the amount of dissolution is time-dependent.

No evidence of direct plagioclase dissolution was observed in calcite-cemented rocks, suggesting that the framework had been protected from migrating fluids. It is likely that dissolution features observed in plagioclase grains in porous rocks resulted from the extensive removal of replacement calcite and, to a lesser extent, from the direct dissolution of feldspar. The relative extent to which these processes have operated is not known, although the indirect removal of plagioclase through dissolution of replacement calcite is far easier to document.

AUTHIGENIC PHYLLOSILICATES

Authigenic clays are dominated by kaolinite, which may form as much as 1 or 2 percent of the total rock volume in porous sandstones. The kaolinite generally occurs as well-crystalized "booklets," which accumulated in the large intergranular pore spaces (fig. 10*E*) and, less commonly, in the intragranular voids of extensively dissolved plagioclase grains. The infrequent development of kaolinite in the intragranular spaces suggests that kaolinite formation is more favored in large, throughgoing pores than in the complex intragranular voids. This aluminous clay commonly occurs in dissolution voids within optically continuous sparry calcite cement. Locally, kaolin developed into very coarse crystals, which may actually replace sparry calcite cement in some rocks. Such crystals are particularly common in the strongly cemented samples of the 29–3X Olson core. The SEM indicates that well-crystalized kaolinite booklets have formed upon quartz overgrowths and on euhedral siderite rhombohedra (fig. 10*D*). All this evidence supports the conclusion that kaolinite formation was among the latest events in the diagenetic history of the Eagle Sandstone. It certainly postdates most calcite formation and dissolution, quartz precipitation, and the formation of iron-rich carbonates. The wide variety of substrates that served for kaolinite growth and its euhedral habit indicate that the clay precipitated directly from dilute migrating pore waters and did not form as an alteration product of preexisting silicates.

Authigenic phyllosilicates other than kaolinite are generally formed only in localized areas. Dominant among these is an iron-rich, mixed-layer illite-smectite clay, containing approximately 80 percent expansible layers. It is most common in samples from the No. 1 Morrison core. This clay occurs as an alteration product of some lithic fragments and as a volumetrically unimportant surface alteration of potassium feldspar. The mixed-layer clay may also occur as sparse pore linings in porous portions of sandstones rich in allogenic clay, and as a flamelike authigenic development upon detrital clays in mudstones. Petrographic evidence and SEM observations similar to those previously described for kaolinite suggest that these clays formed late in the burial history of the Eagle Sandstone. The mixed-layer clay is occasionally associated with kaolinite in pore spaces, but ambiguous morphological relationships between the two clays precludes a relative paragenetic placement for them. The general but not invariable occurrence of the mixed-layer clay with feldspars and allogenic clays, rather than with random open pores in the silicate framework, suggests that locally increased activities of ions other than the alumina and silica required for kaolinite precipitation may have been the controlling factors in its development. No consistent relationship was observed between this mixed-layer clay and framework composition, grain size, sandstone depositional environment, or rock permeability.

Other phyllosilicates are also observed locally in the Eagle Sandstone, although not in the rocks examined in this investigation. These include iron-rich chlorite and highly illitic mixed-layer illite-smectite, which are abundant in the No. 12–1 Blackwood core. To my knowledge, these clays are confined to areas of specifically controlled water chemistry associated with Eocene volcanism, where they may occur with authigenic tourmaline (Gautier, 1979).

SUMMARY OF BURIAL HISTORY

The Eagle Sandstone was deposited along the western shoreline of the Late Cretaceous epicontinental seaway. The sediments were derived from a highland, probably in western Montana, consisting of a mixed terrane of low-grade metasedimentary, sedimentary, volcanic, and possibly plutonic rocks. Clastic materials were transported by fluvial systems through small deltas, and were delivered to the site of deposition by longshore currents. Trace fossils and other textural evidence of bioturbation indicate that the sedimentation interface was aerated during Eagle deposition but that oxygen depletion due to bacterial aerobic respiration must have produced anoxic condi-

tions at very shallow depths in the sediment column. It is likely that a low oxidation potential has persisted in the Eagle Sandstone from that time to the present day.

The formation of concretions and the precipitation of calcite cement began very shortly after burial. This very early carbonate is fine grained and rich in inclusions of organic matter and authigenic pyrite. Inasmuch as bacterial processes in the Eagle Sandstone and associated sediments were probably similar to those observed in the modern marine environment, this pyrite probably developed as a byproduct of the bacterial reduction of sulfate in the anoxic interstitial pore waters. This sulfate reduction was a necessary prerequisite to biogenic methane generation (Claypool and Kaplan, 1974; Presley and Kaplan, 1968). As sedimentation continued and burial depths increased, compaction and minor quartz cementation lithified the uncemented portions of the Eagle Sandstone. By this time quantities of isotopically light methane had been produced by bacterial activity in associated organic-rich sediments. Methane generation continued until compaction precluded bacterial metabolism. However, burial depths were never great enough to induce temperature-related alterations of detrital clays or to achieve detectable thermal maturation of included hydrocarbons. Burial depth probably never exceeded 1,400 m.

Clear, sparry calcite cement began precipitating in intergranular pore spaces, marginally replacing most framework silicates and preferentially replacing many of the abundant plagioclase grains on a large scale. The precise causes and timing of this calcitization are not known. It certainly postdates some compaction and minor quartz cementation. Consistent isotopic fractionation is evident in carbon from this calcite. The calcite has at one time or another occupied virtually every pore and void in the Eagle Sandstone. It is not known with certainty whether this occupation occurred simultaneously throughout the unit, eliminating effective porosity and permeability, or whether it occurred only in discrete layers as at present. I favor the latter view.

Iron-rich carbonates, mainly siderite, formed locally as a result of increased ferrous iron activities, which are usually associated with altering detrital biotite or chlorite fragments. This iron carbonate may have developed as an alteration of preexisting calcite cement. It is likely that the locally extensive formation of isotopically neutral siderite was due to the introduction of iron-rich, bicarbonate-rich waters from outside the stratum.

Intragranular pores presently account for 30 percent or more of the void space in the Eagle Sandstone. Petrographic evidence indicates that most of the pores result from the removal of calcite replacements

of plagioclase. However, at least some direct plagioclase dissolution has occurred.

Authigenic clay minerals, particularly kaolinite, precipitated from solution. Their formation seems to postdate all other diagenetic events and, in the case of kaolin, to be favored in the larger throughgoing pores. The kaolinite may have derived some of its constituent ions from dissolving silicate grains. Locally higher ion activities permitted the formation of compositionally more complex minerals, such as mixed-layer illite-smectite.

Biogenic methane, which formed at very shallow depths early in the burial history of the rocks, must have been present during all phases of diagenesis in the Eagle Sandstone. However, depending upon the interpretation applied to the timing and extent of calcitization, the methane may not have entered its present reservoirs until sometime after the onset of calcite dissolution. Previous work (Gautier, 1979) suggests that at least some major methane migration occurred later than the Eocene tectonic activity and volcanism.

CONCLUSIONS

Results of this investigation suggest that postdepositional processes have affected reservoir properties, as well as hydrocarbon formation and entrapment in the Eagle Sandstone, to a perhaps unexpected extent. Virtually every sample of Eagle Sandstone examined during this study shows evidence that the present size, geometry, and distribution of pores results from diagenetic processes. In addition to the important porosity enhancement resulting from the development of intragranular voids, strong petrographic evidence indicates that most or all of these reservoirs have at one time been extensively occupied by calcite. The timing of this calcitization is not known with certainty, however. The simplest interpretation of this secondary porosity requires that most of the formation was once tightly sealed and thus unable to serve as a reservoir. Alternatively, this dissolution porosity may have been developed through time by mainly localized processes. It is suggested that, at least in the case of conventional methane reservoirs in the Bearpaw Mountains, convincing evidence of secondary porosity is subject to multiple interpretations. In the absence of decisive evidence of simultaneity for the events that produced these effects, their true role in the development of porosity, permeability, and other reservoir properties is an open question.

The present distribution of tightly cemented layers within these

reservoirs limits vertical permeability, thus effectively compartmentalizing the reservoir. If these cemented portions of the reservoirs developed early in the burial history of the Eagle Sandstone, as seems likely at least for some of them, they may have been an important initial trapping mechanism for natural gas. This effect would be of particular importance in lower permeability facies to the east, where preliminary investigations indicate the presence of similar horizontal layers of impermeable sandstone, generally at lithologic breaks.

Authigenic phases potentially hazardous to well completion and treatment procedures have been identified. These include (1) ferrous carbonates, which are easily oxidized to insoluble ferric oxides and hydroxides by the introduction of fluids of relatively high oxidation potential; (2) smectitic mixed-layer clay and intergranular kaolinite, which may expand or migrate in the presence of dilute fluids, and (3) acid-soluble, iron-rich chlorite, the dissolution of which may also facilitate the precipitation of ferric oxides and hydroxides. Chlorite of this type was not observed in this study but has been identified in some Eagle Sandstone reservoirs (Gautier, 1979). Although these minerals may be present in sufficient quantities to affect hydrocarbon exploitation activities, their distribution is not generally predictable. However, intrastratal alterations associated with Eocene volcanism may provide an exception. The extensive formation of authigenic phases observed in the No. 12–1 Blackwood core probably resulted from the introduction of chemically enriched waters associated with volcanic activity (Gautier, 1979). These minerals, which include iron-rich chlorite, highly illitic mixed-layer illite-smectite clay, and quartz and tourmaline, are potentially detrimental to reservoir quality. According to William H. Bayliff (1975, p. 35), wells completed in the Eagle Sandstone near areas of igneous activity in the Bearpaw Mountains display comparatively low initial gas production rates and, subsequently, rapid production decline rates. It is likely that these effects are due to alterations in reservoir sandstones similar to those present in the No. 12–1 Blackwood core.

The extent to which postdepositional processes have operated within shallow gas reservoirs, now occupied by biogenic methane, has not been previously documented. This investigation indicates that the Eagle Sandstone displays many diagenetic features that are similar to those previously observed in rocks having a burial history suitable for the generation of oil or thermogenic gas. I conclude that the thermal maturation of organic matter and deep burial are not prerequisites for the occlusion of porosity by authigenic minerals, nor for the development of significant volumes of secondary intragranular and intergranular porosity.

REFERENCES CITED

Aronson, J. L., and Hower, John, 1976, Mechanism of burial metamorphism of argillaceous sediment—2, Radiogenic argon evidence: Geological Society of America Bulletin, v. 87, p. 738–744.

Baadsgaard, Halfdan, Folinsbee, R. E., and Lipson, J. I., 1961, Potassium-argon dates of biotites from Cordilleran granites: Geological Society of America Bulletin, v. 72, p. 689–702.

Bayliff, W. H., 1975, Performance review of Tiger Ridge and Bullhook gas units, *in* Energy resources of Montana: Montana Geological Society 22d Annual Publication, p. 31–37.

Bogli, Alfred, 1964, Mischungskorrosion—Ein Beitrag zum Verkarstungsproblem: Erdkunde, v. 18, p. 83–92.

Bostick, N. H., 1979, Microscopic measurement of the level of catagenesis of solid organic matter in sedimentary rocks to aid exploration for petroleum and to determine former burial temperatures—A review, *in* Scholle, P. A., and Schluger, P. R., eds., Aspects of diagenesis: Society of Economic Paleontologists and Mineralogists Special Publication no. 26, p. 17–43.

Burst, J. F., Jr., 1959, Postdiagenetic clay mineral environmental relationships in the Gulf Coast Eocene, *in* Swineford, Ada, ed., Clays and clay minerals: National Conference Clays and Clay Minerals, Berkeley, California, 6th, 1957, Proceedings, p. 327–341.

Cairnes, C. E., 1934, Slocan Mining Camp, British Columbia: Canada Geological Survey Memoir 173, 137 p.

Claypool, G. E., and Kaplan, I. R., 1974, The origin and distribution of methane in marine sediments: New York, Plenum Press, p. 99–139.

Garrels, R. M., and Christ, C. L., 1965, Solutions, minerals and equilibria: San Francisco, Freeman, Cooper and Company, 450 p.

Gautier, D. L., 1979, Preliminary report of authigenic, euhedral tourmaline crystals in a productive gas reservoir of the Tiger Ridge field, north-central Montana: Journal of Sedimentary Petrology, v. 49, p. 0911–0916.

Gill, J. R., and Cobban, W. A., 1973, Stratigraphy and geologic history of the Montana Group and equivalent rocks, Montana, Wyoming, and North and South Dakota: U.S. Geological Survey Professional Paper 776, 37 p.

Hayes, J. B., 1979, Sandstone diagenesis—the hole truth, *in* Scholle, P. A., and Schluger, P. R., eds., Aspects of diagenesis: Society of Economic Paleontologists and Mineralogists, Special Publication no. 26, part 2, p. 127–139.

Hayes, J. B., Harms, J. C., and Wilson, T., Jr., 1976, Contrasts between braided and meandering stream deposits, Beluga and Sterling Formations (Tertiary), Cook Inlet, Alaska, *in* Miller, T. P., ed., Recent and ancient sedimentary environments in Alaska: Anchorage, Alaska, Alaska Geological Society, p. J1–J27.

Heald, M. T., and Larese, R. E., 1973, The significance of the solution of feldspar in porosity development: Journal of Sedimentary Petrology, v. 43, p. 453–460.

Hearn, B. C., Jr., 1976, Geologic and tectonic maps of the Bearpaw Mountains area, north-central Montana: U.S. Geological Survey Miscellaneous Geologic Investigations Map I–919.

Helgeson, H. C., 1971, Kinetics of mass transfer among silicates and aqueous solutions: Geochimica et Cosmochimica Acta, v. 35, p. 421–469.

Hoffman, Janet, 1976, Sub-thrust temperatures in the disturbed belt of Montana [abs.]: Geological Society of America Abstracts with Programs, v. 8, p. 196.

Hoffman, Janet, and Hower, John, 1979, Clay mineral assemblages as low grade metamorphic geothermometers—Application to the thrust faulted disturbed belt of Montana, U.S.A., *in* Scholle, P. A., and Schluger, P. R., eds., Aspects of diagenesis: Soci-

ety of Economic Paleontologists and Mineralogists Special Publication no. 26, p. 55–79.

Hoffman, Janet, Hower, John, and Aronson, J. L., 1976, Radiometric dating of time of thrusting in the disturbed belt of Montana: Geology, v. 4, p. 16–20.

Hower, John, and Hall, M. L., 1970, Clay petrology of the Upper Cretaceous Two Medicine Formation, central Montana [abs.]: Clay Minerals Society, Annual Clay Minerals Conference, 19th, Miami Beach, Florida 1970, Program and Abstracts, p. 24.

Hower, John, Eslinger, E. V., Hower, M. E., and Perry, E. A., 1976, Mechanism of burial metamorphism of argillaceous sediment—1, Mineralogical and chemical evidence: Geological Society of America Bulletin, v. 87, p. 725–737.

Klepper, M. R., Weeks, R. A., and Ruppel, E. T., 1957, Geology of the southern Elkhorn Mountains, Jefferson and Broadwater Counties, Montana: U.S. Geological Survey Professional Paper 292, 83 p.

Krauskopf, K. B., 1967, Introduction to geochemistry: New York, McGraw-Hill, 721 p.

Lagache, M., Wyart, J., and Sabatier, G., 1961a, Dissolution des feldspaths alcalins dans l'eau pure ou chargee de CO_2 a 200°C: Academie des Sciences Comptes Rendus, v. 253, p. 2019–2022.

_____1961b, Mechanisme de la dissolution des feldspaths alcalins dans l'eau ou chargee de CO_2 a 200°C: Academie des Sciences Comptes Rendus, v. 253, p. 2296–2299.

Larsen, E. S., Jr., Gottfried, David, Jaffe, H. W., and Waring, C. L., 1958, Lead-alpha ages of the Mesozoic batholiths of western North America: U.S. Geological Survey Bulletin 1070-B, p. 35–62.

Little, H. W., 1960, Nelson map-area, west half, British Columbia: Canada Geological Survey Memoir 308, 205 p.

Maher, P. D., 1969, Eagle gas accumulations of the Bearpaw Mountains area, Montana, *in* Eastern Montana Symposium, 1969: Montana Geological Society 20th Annual Guidebook, p. 121–127.

Mudge, M. R., 1970, Origin of the disturbed belt in northwestern Montana: Geological Society of America Bulletin, v. 8, p. 377–392.

_____1972, Pre-Quaternary rocks in the Sun River Canyon area, northwestern Montana: U.S. Geological Survey Professional Paper 663-A, 142 p.

Mudge, M. R., and Sheppard, R. A., 1968, Provenance of igneous rocks in Cretaceous conglomerates in northwestern Montana: U.S. Geological Survey Professional Paper 600-D, p. 137–146.

Obradovich, J. D., and Cobban, W. A., 1975, A time scale for the Late Cretaceous of the Western Interior of North America, *in* Caldwell, W. G. E., ed., The Cretaceous System of the Western Interior of North America: Geological Association of Canada Special Paper No. 13, p. 31–54.

Perry, Ed, and Hower, John, 1970, Burial diagenesis in Gulf Coast pelitic sediments: Clays and Clay Minerals, v. 18, No. 3, p. 165–177.

Plummer, L. N., 1975, Mixing of sea water with calcium carbonate ground water, *in* Whitten, E. H. T., ed., Quantitative studies in the geological sciences: Geological Society of America Memoir 142, p. 219–236.

Powers, M. C., 1959, Adjustment of clays to chemical change and the concept of equivalence level, *in* Swineford, Ada, ed., Clays and clay minerals: National Confrence Clays and Clay Minerals, 6th, Berkeley, Calif., 1957, Proceedings, p. 309–326.

Presley, B. J., and Kaplan, I. R., 1968, Changes in dissolved sulfate, calcium and carbonate from interstitial water of near-shore sediments: Geochimica et Cosmochimica Acta, v. 32, p. 1037–1048.

Reeves, Frank, 1924, Geology and oil and gas resources of the faulted area south of the Bearpaw Mountains, Montana: U.S. Geological Survey Bulletin 751-C p. 71–114.

_____1946, Origin and mechanics of thrust faults adjacent to the Bearpaw Mountains, Montana: Geological Society of America Bulletin, v. 57, p. 1033–1048.

Rice, D. D., 1975, Origin and significance of natural gases of Montana: U.S. Geological Survey Open-File Report 75-188, 13 p.

_____1980, Coastal and deltaic sedimentation of the Upper Cretaceous Eagle Sandstone and its relation to shallow gas accumulations, north-central Montana: American Association of Petroleum Geologists Bulletin, v. 64, p. 316-338.

Roberts, A. E., 1972, Cretaceous and early Tertiary depositional and tectonic history of the Livingston area, southwestern Montana: U.S. Geological Survey Professional Paper 526-C, 120 p.

Ross, C. P., 1963, The Belt Series in Montana: U.S. Geological Survey Professional Paper 346, 119 p.

Runnells, D. D., 1969, Diagenesis due to the mixing of natural waters—A hypothesis: Nature, v. 224, p. 361-363.

Sabins, F. F., Jr., 1962, Grains of detrital, secondary, and primary dolomite from Cretaceous strata of the Western Interior: Geological Society of America Bulletin, v. 73, p. 1183-1196.

Schmidt, Volkmar, McDonald, D. A., and Platt, R. L., 1977, Pore geometry and reservoir aspects of secondary porosity in sandstones: Bulletin of Canadian Petroleum Geology, v. 25, p. 271-290.

Schorning, Fred, 1972, Reservoir geology of the Tiger Ridge area, *in* Montana Geological Society 21st Annual Field Conference Guidebook, Crazy Mountains Basin, 1972: p. 149-154.

Schultz, L. G., 1964, Quantitative interpretation of mineralogical composition from X-ray and chemical data for the Pierre Shale: U.S. Geological Survey Professional Paper 391-C, 31 p.

_____1978, Mixed-layer clay in the Pierre Shale and equivalent rocks, northern Great Plains region: U.S. Geological Survey Professional Paper 1064-A, 28 p.

Schultz, L. G., Tourtelot, H. A., Gill, J. R., and Boerngen, J. G., 1980, Composition and properties of the Pierre Shale and equivalent rocks, northern Great Plains region: U.S. Geological Survey Professional Paper 1064-B, 114 p.

Smedes, H. W., 1966, Geology and igneous petrology of the northern Elkhorn Mountains, Jefferson and Broadwater Counties, Montana: U.S. Geological Survey Professional Paper 510, 116 p.

Walker, T. R., Ribbe, P. H., and Honea, R. M, 1967, Geochemistry of hornblende alteration in Pliocene red beds, Baja California, Mexico: Geological Society of America Bulletin, v. 787, p. 1055-1060.

Walker, T. R., Waugh, Brian, and Crone, A. J., 1978, Diagenesis in first-cycle desert alluvium of Cenozoic age: Geological Society of America Bulletin, v. 89, p. 19-32.

Weaver, C. E., 1960, Possible uses of clay minerals in search for oil: American Association of Petroleum Geologists Bulletin, v. 44, p. 1505-1518.

Wollast, R., 1967, Kinetics of the alteration of K-feldspars in buffered solutions at low temperature: Geochimica et Cosmochimica Acta, v. 31, p. 635-648.

Zaritskiy, P. V., 1964, Isomorphous entry of $CaC0_3$ into siderite and magnesian siderite concretions of the Donbas: Doklady of the Academy of Sciences, U.S.S.R., Earth Science Sections, v. 155, p. 151-157.

☆U.S. GOVERNMENT PRINTING OFFICE: 1981—576-034/109